

### 3.1 Introduction

---

Crystallization kinetics is the study of rate of change of a highly disordered amorphous structure into an ordered crystalline structure. This study involves every aspect of the conversion from one to other state. In an amorphous alloy, the constituents are trapped in the disordered structure due to super-cooling of the alloy melt. Since these materials are away from equilibrium, the study of their phase transformation becomes crucial to understand the route of formation and to control the structure and properties of amorphous alloys.

The two major reasons to study kinetics of crystallization are:

Firstly, expressing the rate of reaction as a function of state variables, such as temperature, pressure, etc., makes the evaluation of reaction rate easy, though not necessarily accurate, in any other set of conditions. Secondly, it helps to understand the mechanism of reaction. The first kinetic analysis was done by Wilhelmy [3.1], when he tried to study the kinetics of inversion of cane sugar in the presence of acids. He gave the following rate law for the conversion process:

$$-\frac{dx}{dt} = k(C - x) \quad (3.1)$$

Where,  $x$  is the amount of converted cane sugar,  $t$  is the time,  $C$  is the initial amount of cane sugar, and  $k$  is the rate constant. Later on Guldberg and Waage [3.2] and van't Hoff [3.3] also gave rate equations for the reactant to product conversion processes. According to van't Hoff the reaction rate may be written as:

$$-\frac{dC}{dt} = kC^n \quad (3.2)$$

Where,  $C$  is the concentration of each of the reactants,  $t$  is the time and  $n$  is the number of molecules involved in the reaction or the reaction order.

Equation (3.2) holds good for only single step reactions, where all molecules react equally at a time and the reactions of individual molecules remain unaffected by temperature. This limitation of van't Hoff's equation was brought forward by Ostwald [3.4], which motivated further research for multi-step kinetic analysis of thermally activated processes. The general equation for single step reaction was first given by Lewis [3.5]

$$\frac{d\alpha}{dt} = k\alpha(1-\alpha) \quad (3.3)$$

In this expression the concentration was replaced by degree of conversion, since the state of any reacting solid cannot be calculated by its concentration. Soon researchers started analysing multi-step reactions [3.6-3.8] involving two different rate processes for nucleation and growth or nucleation followed by its branching. Bagdassarian [3.9] and Erofeev [3.10] were the first ones to propose multi-step nucleation, which was later generalized by Allnatt and Jacobs [3.11]. Further, growth rate of the nuclei may also differ in different directions. Also different crystals may grow at different rates in a poly-crystal. Hence, occurrence of multi-step reactions is very common and their kinetics cannot be understood by single step reaction mechanism. Following this development in the field of solid-state reaction mechanism, many researchers started working on representing a particular route of a reaction by a reaction model. This representation of reaction mechanism by models was first initiated by Jacobs and Tompkins [3.12]. In eq. (3.3),  $\alpha(1-\alpha)$  can be considered as the reaction model for a particular single-step reaction and thereby giving a general rate equation as:

$$\frac{d\alpha}{dt} = kf(\alpha) \quad (3.4)$$

Eq. (3.4) indicates that the reaction must produce  $\alpha$  versus  $t$  data for a particular degree of conversion. This also implies that, one can use the experimental data of  $\alpha$  versus  $t$  and fit the theoretical data of different models in order to get the real picture of any reaction mechanism.

### **3.1.1 Notion of Activation Energy**

---

All solid state processes need some external force for their activation. These external force may be in terms of temperature, pressure, magnetic field, photo-activation, etc. In present chapter, we will be dealing with the kinetic analysis of activation of solid-state processes by the application of temperature, i.e., thermal activation. Kinetic analysis of a number of thermally driven processes such as thermal oxidation and decomposition of polymers, crystallization of glasses and polymers, solidification of metallic alloys, etc, are available in literature [3.13-3.19]. Dollimore has reported thermal analysis of a wide variety of materials [3.20].

Arrhenius [3.21] brought forward the concept of activation energy that described the reaction rate to be dependent on applied temperature.

$$\frac{d(\log k)}{dT} = \frac{B}{T^2} \quad (3.5)$$

Where,  $T$  is temperature and  $B$  is equal to  $E/R$ , with  $E$  and  $R$  the activation energy and Universal Gas constant ( $8.314 \text{ JK}^{-1}\text{mol}^{-1}$ ).

Equation (3.5) implies:

$$k = k_0 \exp\left(-\frac{E}{RT}\right) \quad (3.6)$$

This is the well-known form of Arrhenius equation, where  $k_0$  is the pre-exponential factor.

Initially,  $E$  was expected to be constant, but later on it was found that the  $E$  values keep on changing with the advancement of reaction. Sometimes this variable nature of  $E$  may introduce some non-linearity in the Arrhenius plot. This non-linearity in Arrhenius plot was first

acknowledged by Hinshelwood [3.22]. This indicates that certain reactions are composed of few reactions running simultaneously at different rates. Though the linear nature of Arrhenius equation has been justified by many researchers, it cannot be generalized for all the solid state processes since it provides an average activation energy for the entire reaction and not for each elementary step occurring in the reaction. Various steps occurring at different rates have their distinct  $E$  value, which gets mixed up when we assume it to be a single-step reaction and a general kinetic data is used to derive a conclusion for the entire process. In such cases, an effective value of  $E$  is obtained which is average of all individual events occurring simultaneously. Eventually, the single-step kinetic analysis turned out to be futile due to two main reasons, i.e., firstly it paid no attention to the experimental variations in activation energy values (the non-linearity in Arrhenius equation) and secondly its tendency to replace the variable  $E$  values for a set of simultaneously occurring events by an average value. Hence, concept of variable activation came into existence.

The kinetics of thermally activated events can be studied either isothermally or non-isothermally. Non-isothermal methods are more frequently used ones as they do not need any time to reach at a particular temperature, unlike isothermal experiments, and the phase transformations occur at their respective temperatures. Moreover, isothermal events have highest reaction rate at its initiation, not allowing the sample to reach high temperatures. Whereas non-isothermal heating can be achieved at very high temperatures also.

### **3.1.2 Kinetics of Phase Change:**

#### **Isokinetic and Iso-conversional Methods**

---

The basic kinetic equation can be written as

$$\frac{d\alpha}{dt} = k(T)f(\alpha) \tag{3.7}$$

Where,  $\alpha$  is the degree of conversion,  $t$  is time,  $k(T)$  is the Arrhenius rate constant (eq. 3.6) and  $f(\alpha)$  is the reaction model. A number of methods are available in literature that evaluate the kinetic parameters ( $E$  and  $k_0$ ) by fitting data to various models ( $f(\alpha)$ ) that are specific to a particular reaction mechanism. These methods are known as “*model fitting methods*” or “*iso-kinetic methods*”. They provide single value of kinetic parameters by assuming the reaction to be same throughout.

The integral form of eq. (3.7) is

$$g(\alpha) \equiv \int_0^{\alpha} [f(\alpha)]^{-1} d\alpha = k(T)t \quad (3.8)$$

This is the case in isothermal conditions. In non-isothermal conditions, time dependence is eliminated by using heating rate ( $\beta$ ) and the above equation takes the following form:

$$g(\alpha) \equiv \int_0^{\alpha} [f(\alpha)]^{-1} d\alpha = \frac{1}{\beta} \int_0^T k(T) dT \quad (3.9)$$

Where,  $\beta$  is  $dT/dt$ .

Equation (3.9) can also be written as

$$g(\alpha) = \frac{k_0}{\beta} \int_0^T \exp\left(-\frac{E}{RT}\right) dT \quad (3.10)$$

Above equation can be used to derive useful information about the kinetic process in terms of the kinetic triplets i.e., the activation energy, pre-exponential factor and the reaction model [3.23].

Iso-kinetic methods, in general, are not applicable to non-isothermal data. They depend upon the reaction model  $f(\alpha)$  for the determination of  $E$  and  $k_0$ . Moreover,  $f(\alpha)$  is found by fitting different reaction models to the experimental data. Also, it provides single vales of Arrhenius parameters. Hence iso-kinetic methods are not appropriate for studying the kinetic process in non-isothermal conditions.

Reliable kinetic parameters can only be measured by the method that does not depend on models, i.e., “*model-free methods*”. These methods are also known as iso-conversional methods. Iso-conversional methods can be used to obtain kinetic parameters by carrying out a series of heating experiments. These methods assume that the reaction rate is a function of temperature only at a particular degree of conversion. Iso-conversional methods are divided into linear and non-linear methods. Linear methods are further bifurcated into differential and integral iso-conversional methods. Linear integral methods are derived using the approximation of the integral term in eq. (3.10). Whereas, differential equations take a differential form as shown below:

$$\left[ \frac{d(\ln(d\alpha / dt))}{dT^{-1}} \right]_{\alpha} = -\frac{E_{\alpha}}{R} \quad (3.11)$$

Vyazovkin and Dollimore [3.24] gave a non-linear method for the calculation of  $E$  with high accuracy. A plenty of linear integral and differential methods are available in literature [3.25-3.32].

Both the methods have their own merits and demerits. Therefore, before performing any analysis, it is essential to confirm the validity of different models by performing some tests, such as: (a) fitting experimental data by theoretical models, Malek test [3.33], Master plots [3.34], etc. In present chapter, different tests have been performed on MDSC data of  $\text{Ti}_{20}\text{Zr}_{20}\text{Cu}_{60}$  metallic glass in order to study the applicability of these methods for studying the non-isothermal crystallization kinetics of metallic glasses.

## 3.2 Theoretical Formulations

---

### 3.2.1 Iso-conversional Methods

---

The reaction rate for non iso-thermal crystallization kinetics can be expressed by the kinetic equation as shown in eq. (3.10) [3.35]. Since, the integral in eq. (3.10) doesn't have an exact analytical solution; various approximations of this integral are suggested in literature [3.36-3.39], for evaluation of activation energies dependent on the degree of conversion,  $\alpha$ .

The general form of the linear equation expressing the linear integral iso-conversional methods is [3.40]:

$$\ln\left(\frac{\beta}{T_\alpha^k}\right) = -A \frac{E_\alpha}{RT_\alpha} + C \quad (3.12)$$

Where  $k$  and  $A$  are parameters depending on approximations of temperature integral,  $C$  is constant and the subscript  $\alpha$  designates the degree of conversion. For Ozawa-Flynn-Wall (OFW) ( $k=0, A=1.0516$ ), Kissinger-Akahira-Sunose (KAS) ( $k=2, A=1$ ) and so on.

#### 3.2.1.1 Linear Iso-conversional Methods

---

##### 3.2.1.1.1 Linear Integral Iso-conversional Methods

---

###### (a) Kissinger-Akahira-Sunose (KAS) Method -The Effect of Non-linearity

Kissinger-Akahira-Sunose (KAS) [3.27-3.28] used the approximation given by Coats and Redfern [3.41] to evaluate the integral in eq. (3.10). This method is based on the expression

$$\ln\left(\frac{\beta}{T_\alpha^2}\right) = -\frac{E_\alpha}{RT_\alpha} + \ln\left(\frac{k_0 R}{E_\alpha}\right) \quad (3.13)$$

The  $E_a$  can be calculated from the slope of the plot  $\ln(\beta/T_a^2)$  vs.  $1000/T_a$  for constant conversion,  $\alpha$ .

For MDSC, the measured heating rate becomes [3.42]

$$\gamma = \beta + A_T \omega \cos \omega t \quad (3.14)$$

Where,  $\beta$  is the linear heating rate and second term is due to sinusoidal temperature modulation.  $A_T$  and  $\omega$  are amplitude and angular frequency ( $2\pi/T$ ;  $T$  is time period) and  $t$  is the time of reaction.

Here, having a positive heating profile is very important to avoid any ambiguity in the measurement of actual heat flow associated with crystallization kinetics. The above condition can be satisfied if,

$$\beta \geq A_T \omega \text{ or, } (A_T \omega / \beta) \leq 1$$

Substituting the heating rate employed by MDSC (eq. (3.14)) in place of  $\beta$  in eq. (3.13), eq. (3.13) becomes

$$\ln\left(\frac{(\beta + A_T \omega \cos \omega t)}{T_a^2}\right) = -\frac{E_a}{RT_a} + \ln\left(\frac{k_0 R}{E_a}\right) \quad (3.15)$$

$$\ln\left(\frac{\beta}{T_a^2} \left(1 + \frac{A_T \omega \cos \omega t}{\beta}\right)\right) = -\frac{E_a}{RT_a} + \ln\left(\frac{k_0 R}{E_a}\right) \quad (3.16)$$

Using properties of ln

$$\ln\left(\frac{\beta}{T_a^2}\right) + \ln\left(1 + \frac{A_T \omega \cos \omega t}{\beta}\right) = -\frac{E_a}{RT_a} + \ln\left(\frac{k_0 R}{E_a}\right) \quad (3.17)$$

Expanding and neglecting higher order terms, we get,

$$\ln\left(\frac{\beta}{T_\alpha^2}\right) + \sum_{n=1}^{\infty} \frac{(-1)^{n+1} \left[\frac{A_T \omega \cos \omega t}{\beta}\right]^n}{n} = -\frac{E_\alpha}{RT_\alpha} + \ln\left(\frac{k_0 R}{E_\alpha}\right) \quad (3.18)$$

$$\ln\left(\frac{\beta}{T_\alpha^2}\right) + \left[\left(\frac{A_T \omega \cos \omega t}{\beta}\right) - \frac{1}{2}\left(\frac{A_T \omega \cos \omega t}{\beta}\right)^2 + \dots\right] = -\frac{E_\alpha}{RT_\alpha} + \ln\left(\frac{k_0 R}{E_\alpha}\right) \quad (3.19)$$

Taking average over 1 complete cycle eq. (3.23) transforms to

$$\ln\left(\frac{\beta}{T_\alpha^2}\right) - \left(\frac{A_T \omega}{2\beta}\right)^2 + \dots = -\frac{E_\alpha}{RT_\alpha} + \ln\left(\frac{k_0 R}{E_\alpha}\right) \quad (3.20)$$

Eq. (3.20) is the KAS equation by using non-linear heating rate of MDSC.

Similar treatment has been done to the linear integral iso-conversional methods i.e., Kissinger method, Augis & Bennett's method, Boswell method, Ozawa-Flynn-Wall (OFW); and linear differential iso-conversional methods i.e., Friedman, and Gao & Wang. The factor  $(A_T \omega / 2\beta)^2$  on L.H.S. of eq. (3.20) is supposed to cause non-linearity.

- i. *Kissinger Method:* This method assumes reaction rate to be maximum at peak temperature ( $T_p$ ). It is used to calculate activation energy at a constant degree of conversion,  $\alpha$  i.e., at  $T_\alpha = T_p$ . Kissinger equation is

$$\ln\left(\frac{\beta}{T_p^2}\right) = -\frac{E}{RT_p} + \ln\left(\frac{k_0 R}{E}\right) \quad (3.21)$$

Kissinger equation for MDSC can be obtained by repeating eq. (3.15) to eq. (3.20) resulting in the final expression:

$$\ln\left(\frac{\beta}{T_p^2}\right) - \left(\frac{A_T \omega}{2\beta}\right)^2 + \dots = -\frac{E}{RT_p} + \ln\left(\frac{k_0 R}{E}\right) \quad (3.22)$$

The slope and intercept the plot  $\ln(\beta/T_p^2)$  vs.  $1000/T_p$  provide the values of activation energy,  $E$  and the pre-exponential factor,  $k_0$  respectively.

- ii. *Augis & Bennett's Method:* This method is an extension of Kissinger method and it is supposed to provide accurate values of kinetic parameters. Apart from peak temperature ( $T_p$ ) it also incorporates onset temperature of crystallization ( $T_o$ ) [3.29].

$$\ln\left(\frac{\beta}{(T_p - T_o)}\right) = -\frac{E}{RT_p} + \ln(k_0) \quad (3.23)$$

For non-linear heating rate, on repeating steps in eq. (3.15) to eq. (3.20) we get,

$$\ln\left(\frac{\beta}{(T_p - T_o)}\right) - \left(\frac{A_r \omega}{2\beta}\right)^2 + \dots = -\frac{E}{RT_p} + \ln(k_0) \quad (3.24)$$

The values of  $E$  and  $k_0$  calculated respectively from the slope and intercept of the plot  $\ln(\beta/(T_p - T_o))$  vs.  $1000/T_p$

- iii. *Boswell Method:* As  $((T_p - T_o)/T_p) \approx 1$ , Augis and Bennett methods may provide crude results. Boswell method, based on the following linear equation [3.30], overcomes the limitation of Augis and Bennett method.

$$\ln\frac{\beta}{T_p} = -\frac{E}{RT_p} + const \quad (3.25)$$

Again following eq. (3.15) to eq. (3.20), for non-linear heating rate, eq. (3.25) modifies to

$$\ln\frac{\beta}{T_p} - \left(\frac{A_r \omega}{2\beta}\right)^2 + \dots = -\frac{E}{RT_p} + const \quad (3.26)$$

The value of  $E$  as calculated from the slope of the plot  $\ln(\beta/T_p)$  vs.  $1000/T_p$ .

**(b) Ozawa-Flynn-Wall (OFW) Method**

Ozawa-Flynn-Wall [3.25-3.26] solved eq. (3.10) by using Doyle's approximation [3.42-3.45].

The OFW expression is

$$\ln \beta = -1.0516 \frac{E_{\alpha}}{RT_{\alpha}} + const \quad (3.27)$$

Following steps (3.15) to (3.20) for eq. (3.27) we get

$$\ln(\beta) - \left(\frac{A_r \omega}{2\beta}\right)^2 + \dots = -1.0516 \frac{E_{\alpha}}{RT_{\alpha}} + const \quad (3.28)$$

At  $T_{\alpha}=T_p$  (Ozawa method) the value for activation energy is determined using eq. (3.27) and its modified expression for non-linear heating rate is obtained by replacing  $T_{\alpha}=T_p$  in eq. 3.28.

**3.2.1.1.2 Linear Differential Iso-conversional Methods**

---

These methods use the differential of the transformed fraction to calculate the activation energy,  $E_{\alpha}$ . From eq. (3.7) Friedman [3.31] derived a linear differential iso conversional expression

$$\ln\left(\frac{d\alpha}{dt}\right)_{\alpha} = \ln \beta \left(\frac{d\alpha}{dT}\right)_{\alpha} = -\frac{E_{\alpha}}{RT_{\alpha}} + \ln(k_0 f(\alpha)) \quad (3.29)$$

This method is also supposed to give accurate results of  $E$ , since it does not apply any mathematical approximation to the temperature integral. However, since it is a differential method its accuracy is limited by signal noise.

Eq. (3.29) can be modified to eq. (3.30) by repeating eq. (3.15) to eq. (3.20),

$$\ln \beta \left( \frac{d\alpha}{dT} \right)_\alpha - \left( \frac{A_T \omega}{2\beta} \right)^2 + \dots = -\frac{E_\alpha}{RT_\alpha} + \ln(k_0 f(\alpha)) \quad (3.30)$$

The values of  $E$  can be calculated from the slope of the plot  $\ln (\beta (d\alpha/dT)_\alpha)$  vs.  $1000/T_\alpha$  for constant conversion,  $\alpha$

A method suggested by Gao & Wang [3.32] is a special case of Friedman method. The expression used by Gao & Wang is as followed

$$\ln \left( \beta \frac{d\alpha}{dT_p} \right) = -\frac{E}{RT_p} + const \quad (3.31)$$

For non-linear heating rate, again by performing steps in eq. (3.15) to eq. (3.20), eq. (3.31) changes to

$$\ln \left( \beta \frac{d\alpha}{dT_p} \right) - \left( \frac{A_T \omega}{2\beta} \right)^2 + \dots = -\frac{E}{RT_p} + const \quad (3.32)$$

The values of  $E$  can be calculated from the slope of the plot  $\ln (\beta (d\alpha/dT_p))$  vs.  $1000/T_p$ .

### 3.2.2 Iso-kinetic Methods

---

Most of the iso-kinetic methods are based on the KJMA rate equation [3.46-3.50] given by

$$\frac{d\alpha}{dt} = nk(1-\alpha) [-\ln(1-\alpha)]^{(n-1)/n} \quad (3.33)$$

Where  $\alpha$  is degree of conversion at a particular time  $t$ ,  $n$  is Avrami (growth) exponent and  $k$  is the Arrhenius rate constant given by eq. (3.6)

From equations (3.33) & (3.6) transformed fraction can be expressed as

$$\alpha = 1 - \exp \left[ -\frac{k_0}{\beta} \int_{T_0}^T \exp \left( -\frac{E}{RT} \right) dT \right]^n \quad (3.34)$$

The integral in eq. (3.13) does not have an exact solution and hence one has to switch to approximations. Various approximations have been used in literature to obtain an accurate solution of the integral [3.51-3.53]. On employing Gorbachev approximation [3.53] i.e., eq. (3.35) in eq. (3.34) we obtain eq. (3.36).

$$\int_0^T e^{-E/RT} dT = \frac{RT^2}{E + 2RT} e^{-E/RT} \quad (3.35)$$

$$\alpha = 1 - \exp \left[ -\left\{ \frac{k_0 RT^2}{\beta(E + 2RT)} \exp \left( -\frac{E}{RT} \right) dT \right\}^n \right] \quad (3.36)$$

The values of  $E$ ,  $n$  and  $k_0$  can be determined by fitting the experimental data of  $\alpha$  to eq. (3.36) with the help of method of least square.

### 3.2.3 Testing Techniques

---

In order to get realistic values of kinetic parameters  $E$  and  $k_0$ , one must test the validity of different models then use suitable method for interpretation of kinetic data.

#### 3.2.3.1 Malek Test

---

The validity of KJMA model in non-isothermal conditions can be checked by various methods available in literature [3.33, 3.54-3.55]. Malek [3.33] proposed a simple method for checking the applicability of KJMA model. According to Malek the KJMA model is valid for studying the non-isothermal crystallization kinetics if the maximum of the function  $z(\alpha)$  comes in the

range (0.61-0.65). In present study we have calculated both  $y(\alpha)$  and  $z(\alpha)$  as expressed in eq. (3.37) and (3.38) respectively.

$$y(\alpha) = \phi \exp(E/RT) \quad (3.37)$$

$$z(\alpha) = \phi T^2 \quad (3.38)$$

Where  $\phi$  is the heat flow evaluated during the crystal growth, represented by the following equation

$$\phi = \Delta H_c k_0 \exp(-E/RT) f(\alpha) \quad (3.39)$$

And

$$f(\alpha) = n(1-\alpha) [-\ln(1-\alpha)]^{(n-1)/n} \quad (3.40)$$

Where,  $\Delta H_c$  is the enthalpy difference associated with crystallization process.

If  $0 < \alpha_M < \alpha_P$  (where  $\alpha_M$  and  $\alpha_P$  are maximum of  $y(\alpha)$  and  $z(\alpha)$  respectively), and  $\alpha_P$  is not equal to zero, then Malek's criteria suggests the equation for  $f(\alpha)$  given by Sestak-Berggren [3.56], used for evaluating the kinetic parameters.

Sestak-Berggren equation is given as:

$$f(\alpha) = \alpha^M (1-\alpha)^N \quad (3.41)$$

Where,  $M$  and  $N$  are kinetic parameters, their ratio can be calculated as:

$$\frac{M}{N} = \frac{\alpha_M}{(1-\alpha_M)} \quad (3.42)$$

Considering S-B equation, the reaction rate can be given as:

$$\frac{d\alpha}{dt} = Z \exp\left(-\frac{E_\alpha}{RT}\right) \alpha^M (1-\alpha)^N \quad (3.43)$$

Another way of representing SB equation is:

$$\ln\left[\left(\frac{d\alpha}{dt}\right) \exp\left(\frac{E_\alpha}{RT}\right)\right] = \ln Z + N \ln\left[\alpha^{M/N} (1-\alpha)\right] \quad (3.44)$$

The value of  $N$  can be obtained from the slope of the plot  $\ln[(d\alpha/dt) \exp(E_\alpha/RT)]$  versus  $\ln[\alpha^{M/N}(1-\alpha)]$ . The parameter  $M$  can then be calculated from equation (3.42).

### 3.2.3.2 Master Plot

---

For a more precise check of the above determined kinetic parameters, Master plot and heat flow curve match can be performed. In master plot method [3.34], considering  $\alpha=0.5$ , the experimental and theoretical values of the appropriate reaction model can be compared by applying the following equation:

$$\frac{f(\alpha)}{f(0.5)} = \frac{d\alpha/dt}{(d\alpha/dt)_{0.5}} \frac{\exp(E_\alpha/RT)}{\exp(E_\alpha/RT_{0.5})} \quad (3.45)$$

The left side of the expression represents the theoretically calculated reduced reaction model with respect to the reaction function at  $\alpha=0.5$ . The right side of the expression is calculated from the experimentally determined values of activation energy.

### 3.2.3.3 Normalized Heat Flow Curves

---

For a more rigorous check of applicability of KJMA equation, we have obtained the theoretical normalized heat flow curves by making use of calculated kinetic parameters i.e.,  $E$  and  $n$  and equations (3.39) and (3.40). The values of local Avrami exponent are calculated using the following equation [3.57]

$$n(\alpha) = -\frac{R}{E(\alpha)} \frac{\partial \ln[-\ln(1-\alpha)]}{\partial(1/T)} \quad (3.46)$$

### 3.3 Concept of Crystallization temperature

---

Metallic glasses exhibits some characteristics temperatures i.e., the glass transition temperature ( $T_g$ ), the onset of crystallization temperature ( $T_x$ ), melting temperature ( $T_m$ ), etc, when they are subjected to thermal treatment. These temperatures symbolize the commencement of various phase changes occurring in the amorphous alloy, such as  $T_g$ ,  $T_x$ , and  $T_m$  indicates the initiation of glass transition, crystallization, and melting processes. The crystallization temperature ( $T_x$ ) represents the onset of crystallization process and the peak crystallization temperature ( $T_p$ ) represents the temperature of the peak of crystallization event. Both  $T_x$  and  $T_p$  shows a significant variation with heating rate ( $\beta$ ). In order to study the kinetic nature of these transition temperatures, the variation of  $T_x$  and  $T_p$  with heating rate is studied for Cu-based metallic glasses. The information about  $T_x$  and  $T_p$  at different heating rates help in finding the activation energy of crystallization for metallic glasses by the use of various iso-kinetic and iso-conversional methods as discussed in the previous sections. Further, the effect of substitution of Ti for Zr in  $\text{Cu}_{60}\text{Zr}_{40}$  metallic glass is also discussed in terms of  $T_x$ .

#### 3.3.1 Variation of $T_x$ and $T_p$ with Heating Rate

---

For understanding the crystallization behaviour and thermal stability of metallic glasses, it is crucial to understand the relationship between the crystallization temperatures and the applied heating rate. Many relations are available in literature to study temperature variation with heating rate, such as Kissinger equation, Ozawa equation, Lasocka equation, etc [3.25-3.30, 3.58-3.59]. Most of the methods suggest linear relationship of  $T_x$  and heating rate, but this may not be true for all the cases. Both  $T_x$  and  $T_p$  shows a significant variation with heating rate ( $\beta$ ).

$T_x$  and  $T_p$  are shifted to higher temperatures with increasing heating rates, which implies that crystallization depends upon heating rate during continuous heating [3.60-3.61].

The variation of crystallization temperature with heating rates can be understood in terms of power law equation [3.58], i.e,

$$T_x = T_0 [\beta]^y \quad (3.47)$$

Where,  $\beta$  is the normalized heating rate,  $T_0$  is the  $T_x$  at a heating rate of  $1^{\circ}\text{Cmin}^{-1}$ . Normalization has been done with respect to heating rate of  $1^{\circ}\text{C min}^{-1}$ .

Using eq. (3.47) exponent  $y$  can be calculated as

$$y = \log_{10} \left[ \frac{(T_x)_\alpha}{(T_x)_1} \right] [\log_{10} [\beta]]^{-1} \quad (3.48)$$

Where  $(T_x)_\alpha$  represents  $T_x$  at any arbitrary heating rate. In present study, we have taken  $\alpha = 4$ , i.e.,  $T_x$  at  $4^{\circ}\text{C min}^{-1}$ . And  $(T_x)_1$  represents  $T_x$  at  $1^{\circ}\text{C min}^{-1}$  (i.e.,  $T_0$ ).

In a similar way  $T_p$  variation with  $\beta$  can be written as

$$T_p = T_0 [\beta]^y \quad (3.49)$$

Where  $y$  can be calculated as

$$y = \log_{10} \left[ \frac{(T_p)_\alpha}{(T_p)_1} \right] [\log_{10} [\beta]]^{-1} \quad (3.50)$$

Here,  $(T_p)_\alpha$  and  $(T_p)_1$  are value of  $T_p$  at  $4^{\circ}\text{C min}^{-1}$  and  $1^{\circ}\text{C min}^{-1}$  respectively.

### 3.4 Results and Discussions

---

Cu-Zr-Ti alloys are found to have excellent thermal and mechanical properties [3.62-3.63].

Among various compositions of Cu-Zr-Ti alloys,  $\text{Ti}_{20}\text{Zr}_{20}\text{Cu}_{60}$  is found to have highest glass

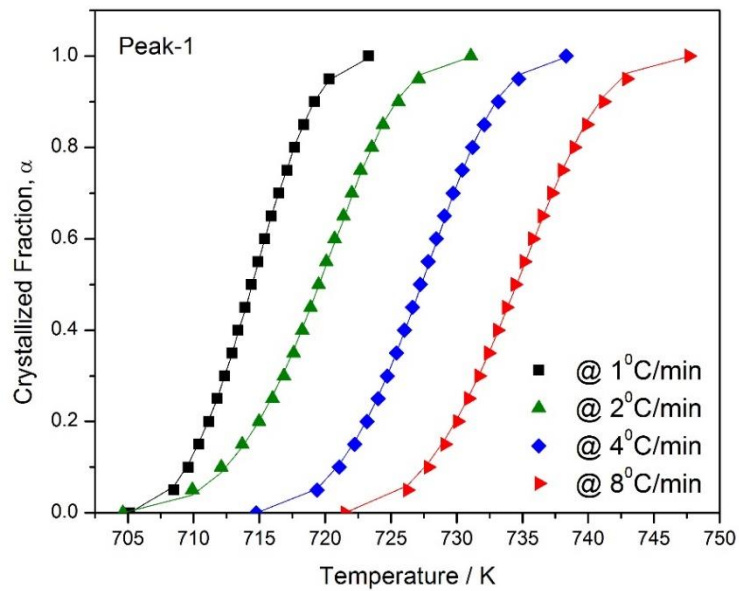
forming ability (GFA) [3.62]. Due to its high glass forming ability, various studies have been carried out on this metallic glass for understanding its crystallization kinetics [3.64-3.66]. Hence, in present case, we have studied non iso-thermal crystallization of  $Ti_{20}Zr_{20}Cu_{60}$  metallic glass.

The modulated DSC experiments clearly indicate two step crystallization process. The crystallized fraction,  $\alpha$  was calculated from MDSC curves and variation of  $\alpha$  with temperature, at all the studied heating rates, is shown in fig. 3.1(a) & fig. 3.1(b) for the two crystallization peaks respectively. Iterative least-square fitting method was used to fit the experimental data of fractional crystallization to eq. (3.36). Kissinger equation was used to obtain the initial estimates of  $E$  and  $k_0$ . The sigmoidal variation of crystallized fraction ( $\alpha$ ), with temperature indicates that crystallization is occurring in bulk. Table 3.1 reports the values of  $E$ ,  $k_0$ , and  $n$  obtained by least square fitting method.

Table 3.1 Values of Avrami (growth) exponent ( $n$ ), pre-exponential factor ( $k_0$ ) and activation energy ( $E$ ) obtained by least square fitting of fractional crystallization data for both the crystallization peaks.

<b>Heating Rate (<math>^{\circ}Cmin^{-1}</math>)</b>	<b>KJMA (Eq. (3.36))</b>					
	<b>Peak 1</b>			<b>Peak 2</b>		
	$n$	$k_0 (10^{22} s^{-1})$	$E (kJmol^{-1})$	$n$	$k_0 (10^{17} s^{-1})$	$E (kJmol^{-1})$
1	1.91	1.12	338	2.34	3.44	287
2	1.93	4.27	346	2.00	2.28	284
4	1.90	1.33	338	2.08	1.85	282
8	1.77	1.05	336	2.01	1.46	280

(a)



(b)

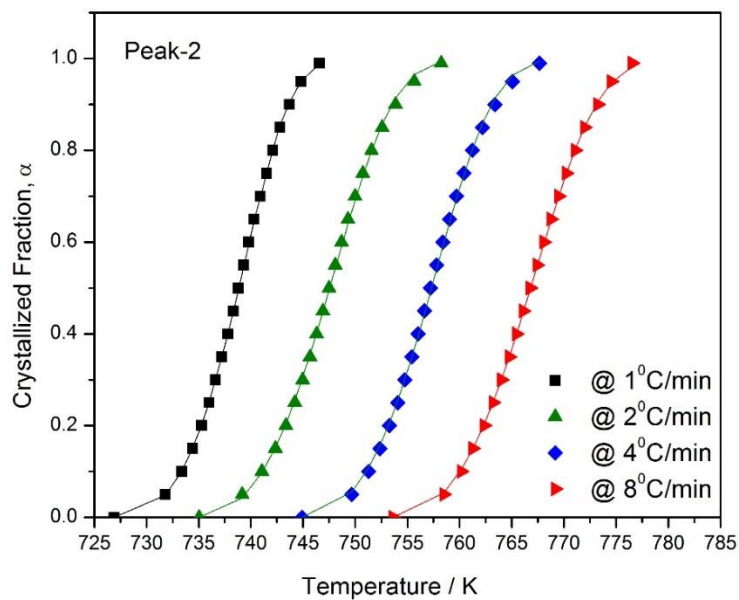
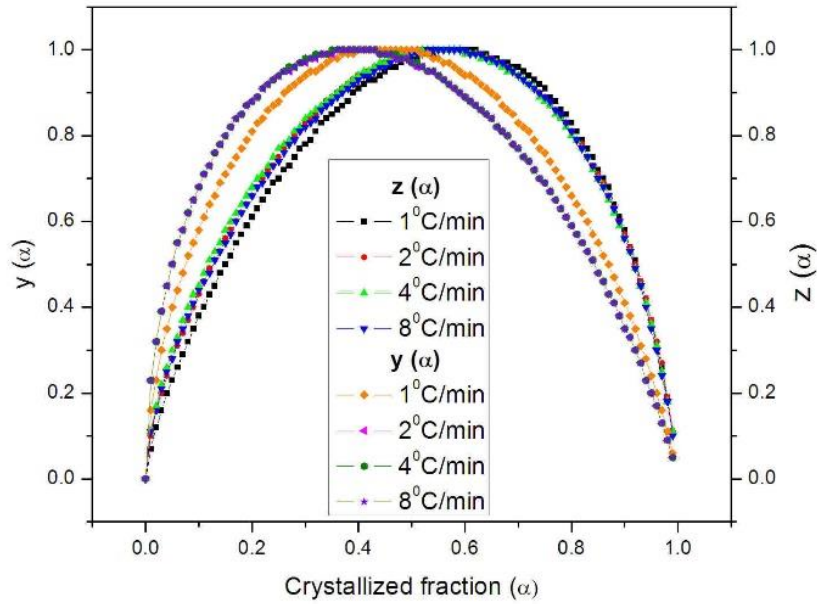


Fig. 3.1: Crystallized fraction as a function of temperature for  $Ti_{20}Zr_{20}Cu_{60}$  metallic glass at different heating rates; (a) Peak-1, (b) Peak-2: symbols represent experimental points and solid lines show the least square fitted curve using eq. (3.36)

Figure 3.2 represents the variation of  $y(\alpha)$  and  $z(\alpha)$  with crystallized fraction  $\alpha$ . As shown in the plots, the maximum of  $z(\alpha)$  falls in the range (0.50 - 0.59) and (0.55 – 0.60) for peak 1 and 2 respectively, whereas that of  $y(\alpha)$  falls in the range (0.27 – 0.35) and (0.38 – 0.45) respectively for peak 1 and 2. These values are less than that predicted by Malek [3.33]. Hence in present case, KJMA model cannot be used for the study of non-isothermal crystallization kinetics.

Figures 3.3(a) - (h) represent the experimental normalized heat flow and the theoretically calculated normalized heat flow using equations (3.39) and (3.40). For iso-kinetic methods the values of  $E$ ,  $n$ , and  $k_0$  used, are those obtained from the least square fitting method and are listed in table 3.1. For iso-conversional methods,  $E$  and  $k_0$  values used are calculated by KAS method.

(a)



(b)

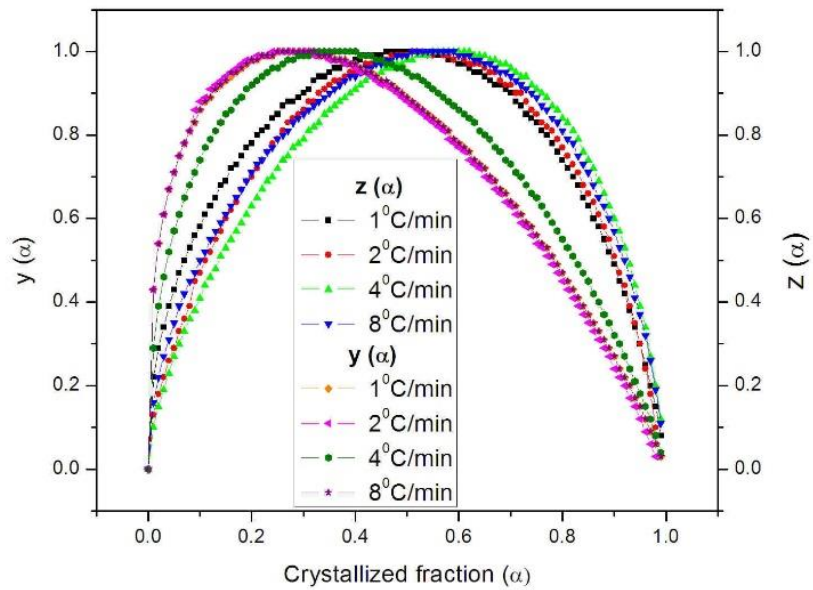
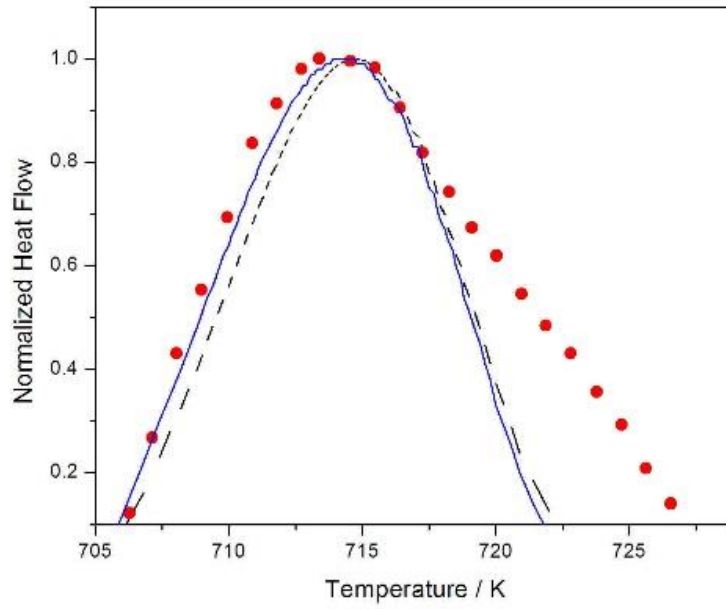
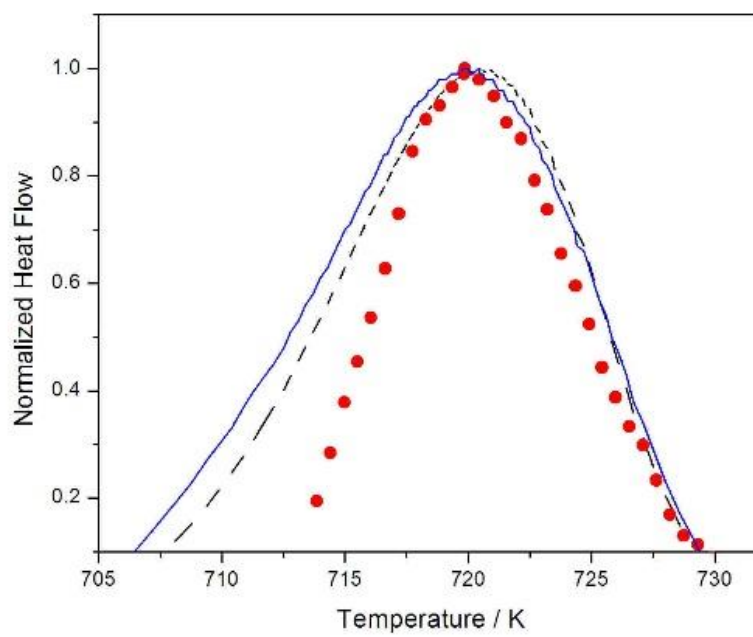


Fig. 3.2: Normalized  $y(\alpha)$  and  $z(\alpha)$  with crystallized fraction  $\alpha$  for different heating rates; (a) Peak-1, (b) Peak-2

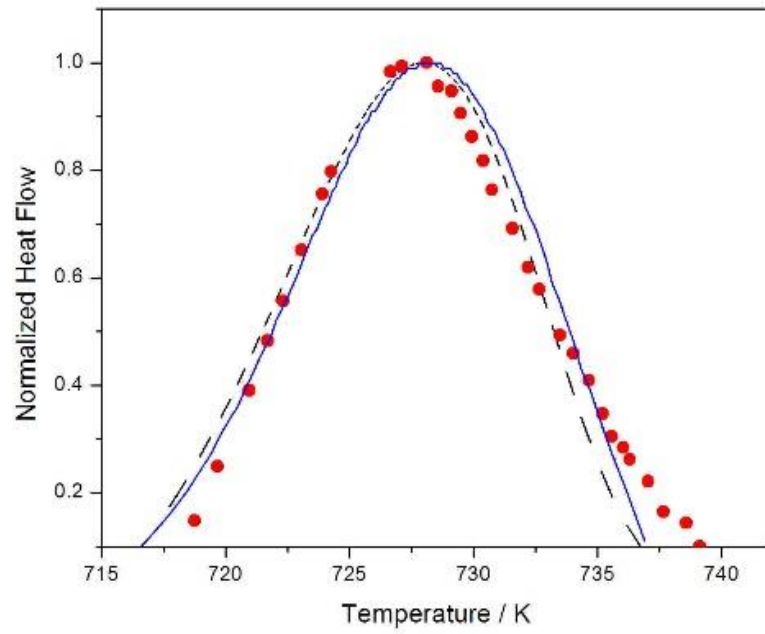
(a)



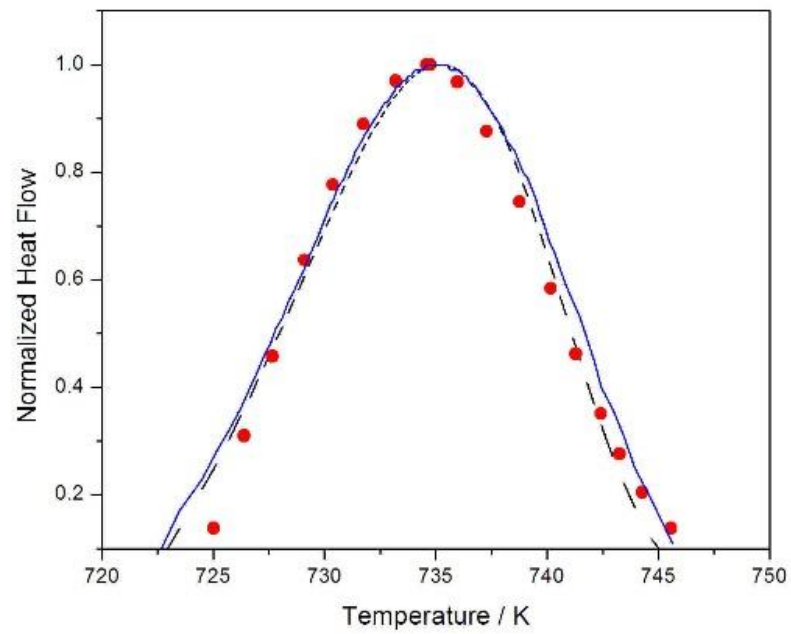
(b)



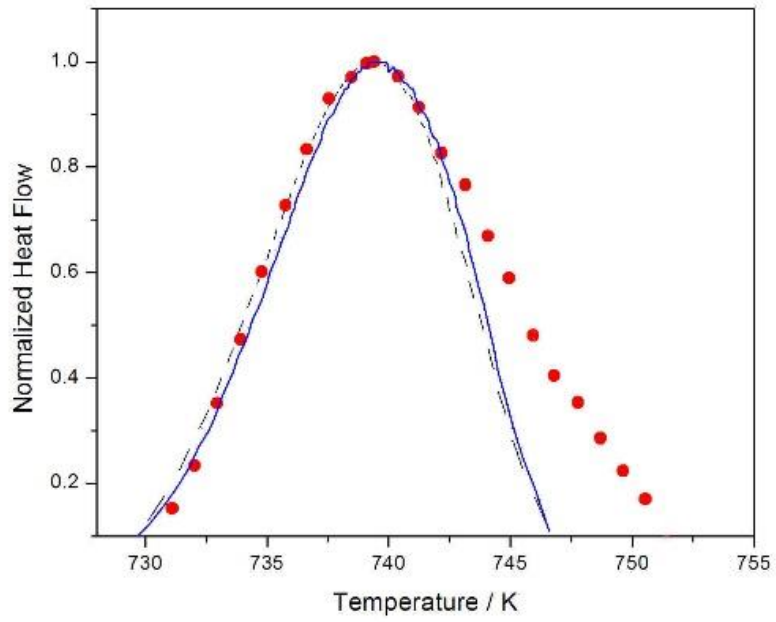
(c)



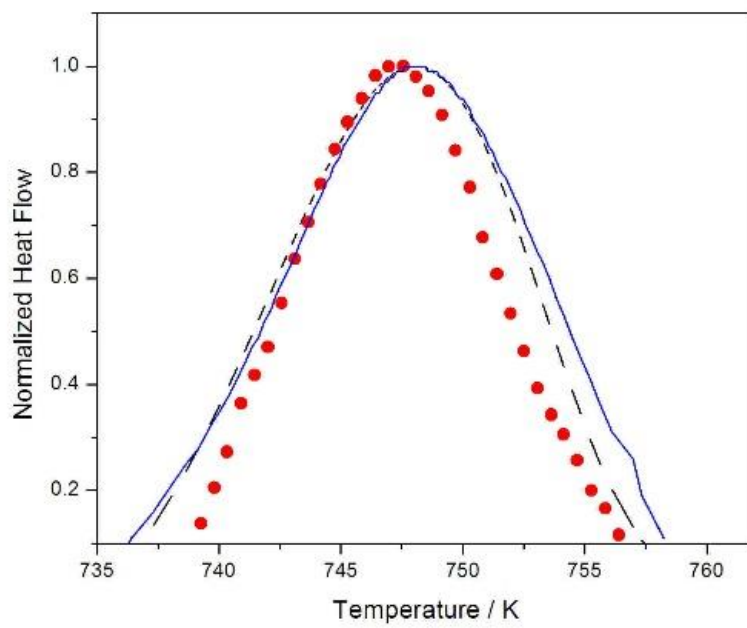
(d)



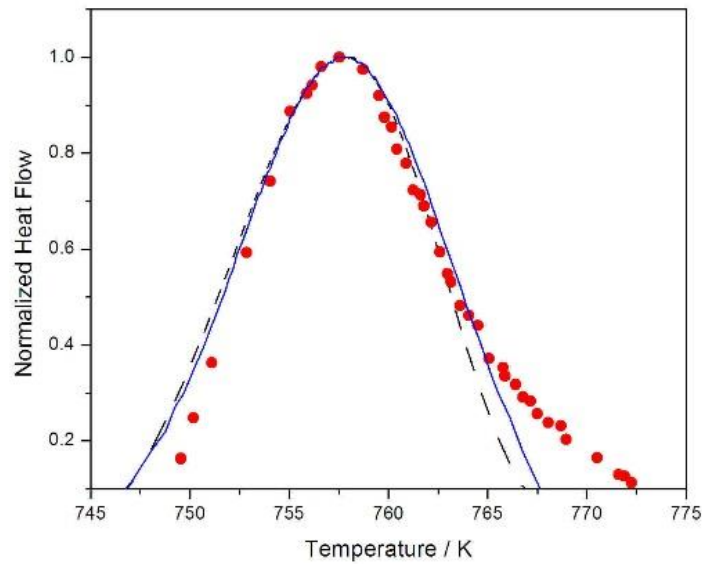
(e)



(f)



(g)



(h)

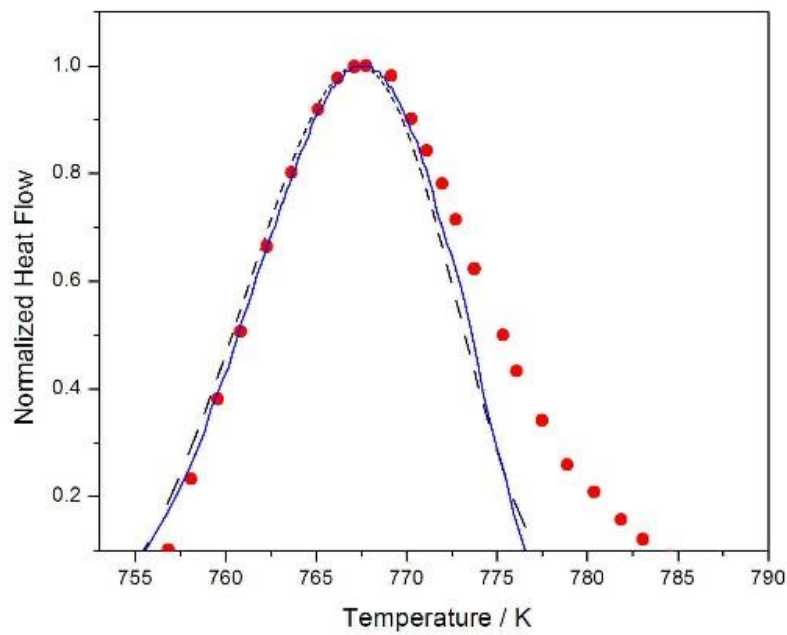


Fig. 3.3: Normalized heat flow curves at different heating rates; (••••) experimental, (- - -) iso-kinetic results, (—) iso-conversional results.(a-d) Peak-1: (a) 1°Cmin<sup>-1</sup>, (b) 2°Cmin<sup>-1</sup>, (c) 4°Cmin<sup>-1</sup>, (d) 8°Cmin<sup>-1</sup>; (e-h) Peak-2: (e) 1°Cmin<sup>-1</sup>, (f) 2°Cmin<sup>-1</sup>, (g) 4°Cmin<sup>-1</sup>, (h) 8°Cmin<sup>-1</sup>

It can be seen from figures 3.3 (a)-(h) that iso-conversional and iso-kinetic methods show a close match to each other. Both of them show a deviation from the experimental data at lower heating rates. As heating rate increases, the theoretically calculated normalized heat flow values matches with the experimental data. Further, for all heating rates the calculated values deviate at both the tails of the peak, but show a close match in intermediate temperature range. This deviation at the peak tails may be due to high errors in the base line interpolation for peak tails [3.33]. It can also be noted that before peak crystallization temperature the normalized heat flow calculated by iso-conversional method matches more accurately with the experimental results, except for fig 3.3(b). After the near peak region, the iso-kinetic method provides better results. It can be understood in terms of nucleation and growth processes. During initial stages of crystallization process nucleation and growth occur simultaneously, but after the peak nucleation process becomes negligible and crystallization is dominated by growth process. Thus, the entire crystallization process is a complex phenomenon and hence it cannot be explained completely by iso-kinetic methods. For understanding this complex process, the dependence of  $E$  on  $\alpha$  is studied by various iso-conversional methods.

### **3.4.1 Linear Integral Iso-conversional Methods**

The variable values of  $E_\alpha$  and the  $k_0$  are calculated at different degree of conversion ( $\alpha$ ) by using KAS and OFW methods, and the values are shown in table 3.2. Fig. 3.4 (a) & (b) and Fig. 3.5 (a) & (b) shows the KAS and OFW plots for both the crystallization peaks.

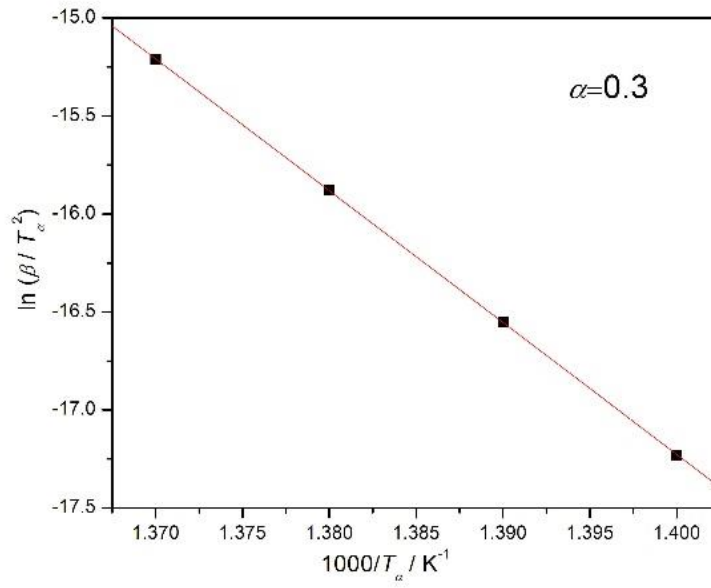
The factor  $(A_T\omega/2\beta)^2$  on L.H.S. of eq. (3.20) is coming out to be almost constant for all heating rates. Hence, its contribution to non-linearity is negligible, which is clearly indicated by figures 3.4(a) & 3.4(b). Typically  $(A_T\omega/\beta) \approx 1$ , for e.g., for  $\beta = 1^{\circ}\text{C}/\text{min}$ ,  $A_T = 0.16$ ,  $\omega = (2\pi)/p$ , where  $p$  is time period ( $=60\text{ s}$ );  $(A_T\omega/\beta) = 1$ .

Table 3.2 Local activation energies ( $E_a$ ) at different degrees of conversions,  $\alpha$  for different methods

$\alpha$	$E_a$ (kJ/mol)					
	KAS		OFW		Friedman	
	Peak-1	Peak-2	Peak-1	Peak-2	Peak-1	Peak-2
0.1	418 ± 6	390 ± 5	407 ± 7	383 ± 5	420 ± 3	342 ± 1
0.2	393 ± 5	341 ± 4	383 ± 5	337 ± 4	409 ± 3	335 ± 1
0.3	559 ± 0	321 ± 4	548 ± 0	316 ± 7	403 ± 2	329 ± 1
0.4	415 ± 7	320 ± 4	407 ± 7	316 ± 7	392 ± 0	318 ± 1
0.5	418 ± 7	319 ± 4	407 ± 7	316 ± 4	417 ± 4	306 ± 1
0.6	392 ± 5	321 ± 4	383 ± 5	316 ± 4	385 ± 1	306 ± 1
0.7	433 ± 7	341 ± 4	407 ± 7	337 ± 4	369 ± 1	307 ± 1
0.8	416 ± 7	319 ± 4	407 ± 7	316 ± 4	365 ± 1	296 ± 2
0.9	392 ± 5	319 ± 4	383 ± 5	316 ± 4	355 ± 2	305 ± 5
1	390 ± 5	320 ± 4	383 ± 5	316 ± 4	304 ± 4	358 ± 7

Isoconversional methods also includes some methods that provide  $E$  values only at the peak crystallization temperature ( $T_p$ ). These methods include Kissinger method [3.27], Augis-Bennette method [3.29], Boswell method [3.30], Ozawa method [3.25], etc. The reaction rate is assumed to be highest at the peak crystallization temperature, hence, if the value of  $E$  is known at that temperature, entire crystallization process can be controlled in order to achieve desired degree of crystallinity.

(a)



(b)

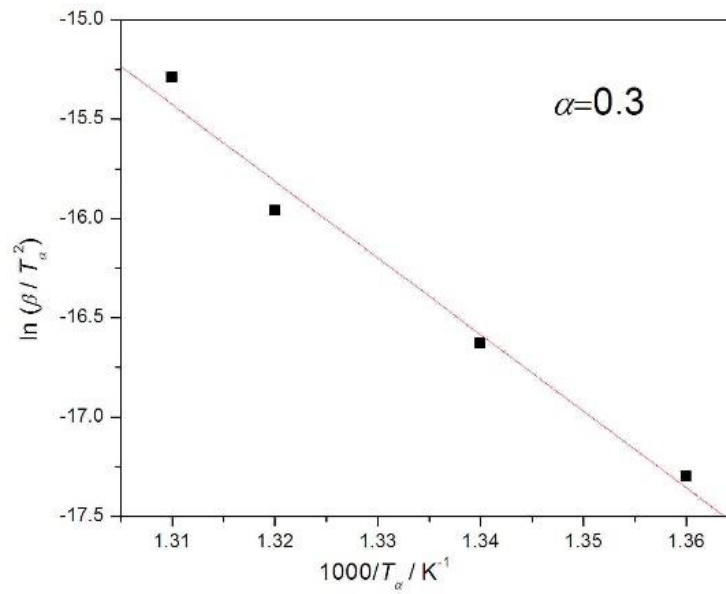
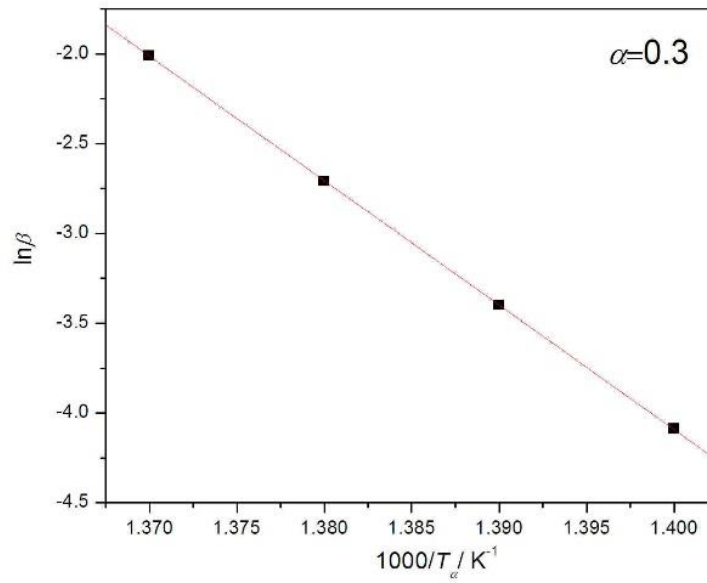


Fig. 3.4: KAS plot for  $\alpha = 0.3$ ; (a) Peak-1, (b) Peak-2

(a)



(b)

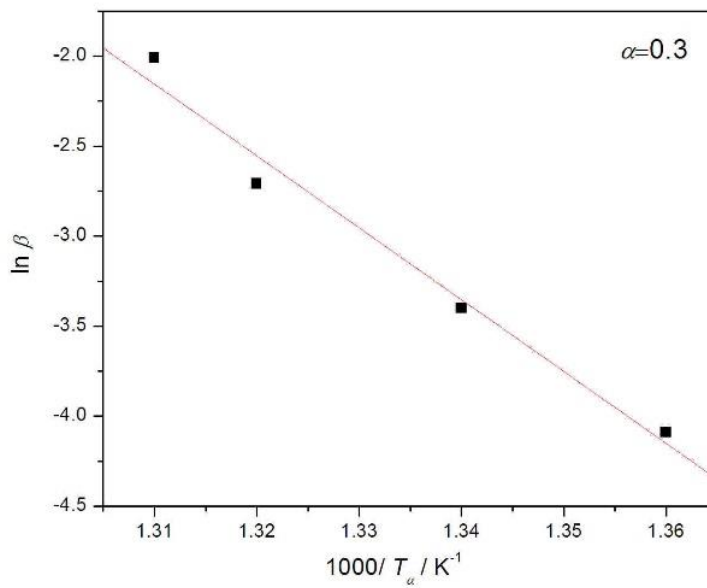
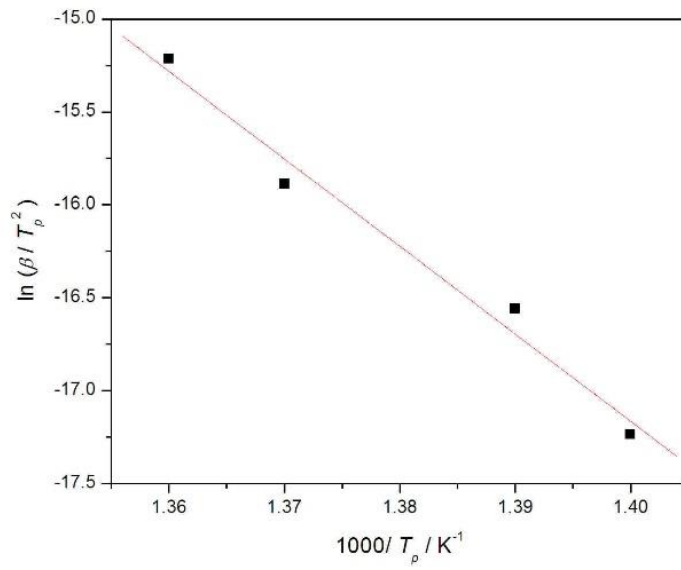


Fig. 3.5: OFW plot for  $\alpha = 0.3$ ; (a) Peak-1, (b) Peak-2

Kissinger equation calculates activation energy at a constant  $\alpha$  i.e., at  $T_{\alpha} = T_p$  only using equation (3.21). For non-linear heating rate equation 3.22 is used to calculate  $E$  and  $k_0$  values, and the so obtained values are reported in table 3.3. Fig. 3.6 (a) & (b) shows Kissinger plots for first and second peak respectively. Augis & Bennett equation subsumes the onset of crystallization temperature ( $T_0$ ) along with the  $T_p$ . Equation (3.24) represents the Augis & Bennett equation for non-linear heating rate, and its plots are shown in fig 3.7 (a) & (b) for both peaks. This method is also applicable to heterogeneous reactions. But, as  $((T_p - T_0)/T_p) \approx 1$ , it may provide crude results. This limitation of Augis & Bennett method is overcome by Boswell method, which is shown in eq. (3.26). Boswell plots for both crystallization process are shown in fig 3.8 (a) & (b). Ozawa method is a special case of OFW method, which finds  $E$  values only at  $T_p$ . Ozawa plots are shown in fig. 3.9 (a) & (b) for both peaks calculated by using eq. (3.28). The values of  $E$  and  $k_0$  obtained by Augis & Bennett, Boswell, and Ozawa methods are shown in table 3.3.

(a)



(b)

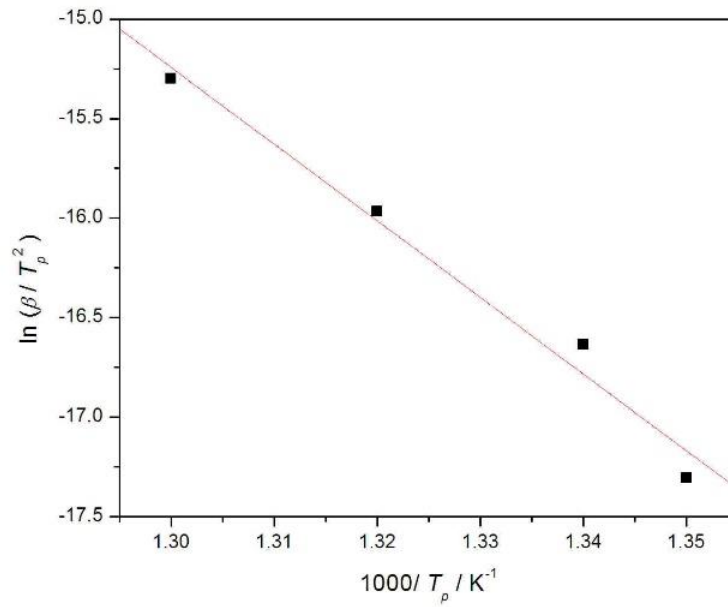
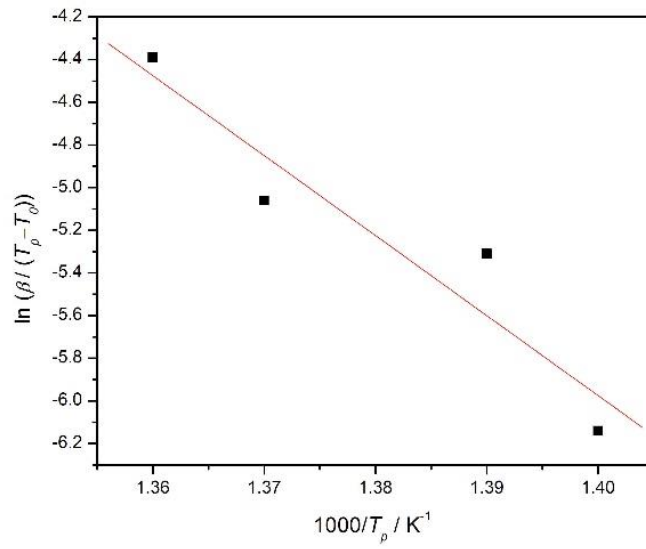


Fig. 3.6: Kissinger plot; (a) Peak-1, (b) Peak-2

(a)



(b)

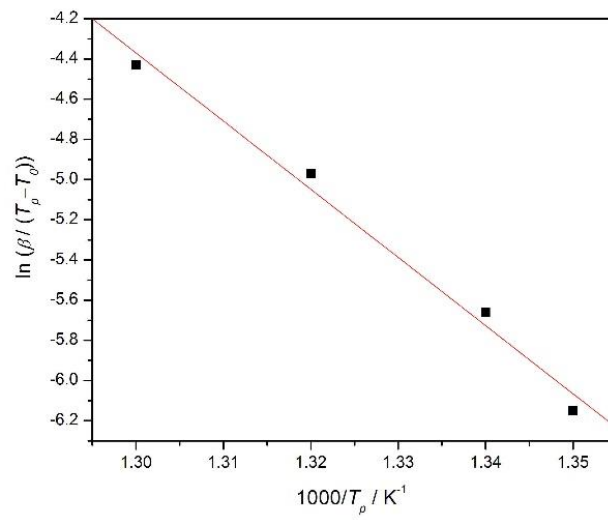
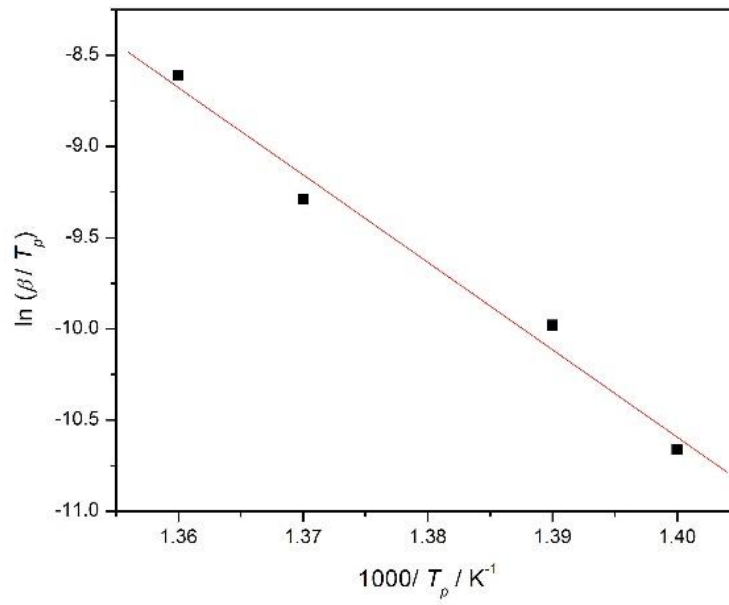


Fig. 3.7: Augis & Bennett's plot; (a) Peak-1, (b) Peak-2

(a)



(b)

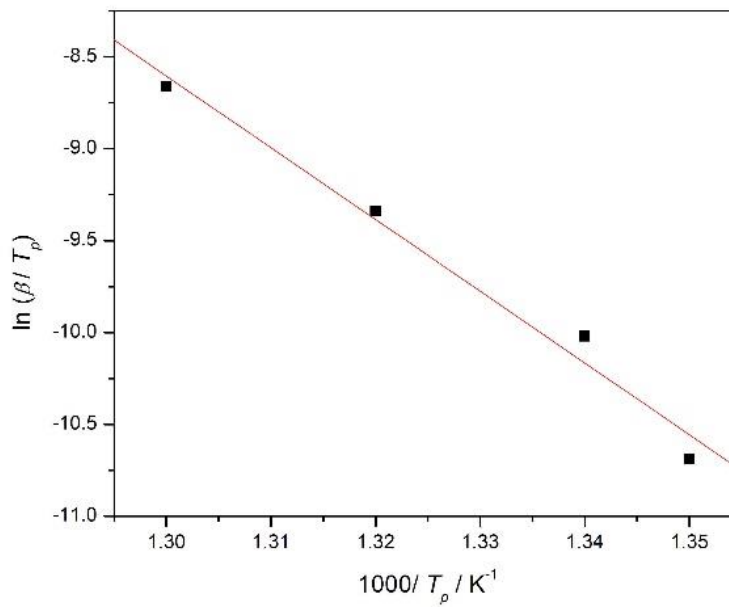
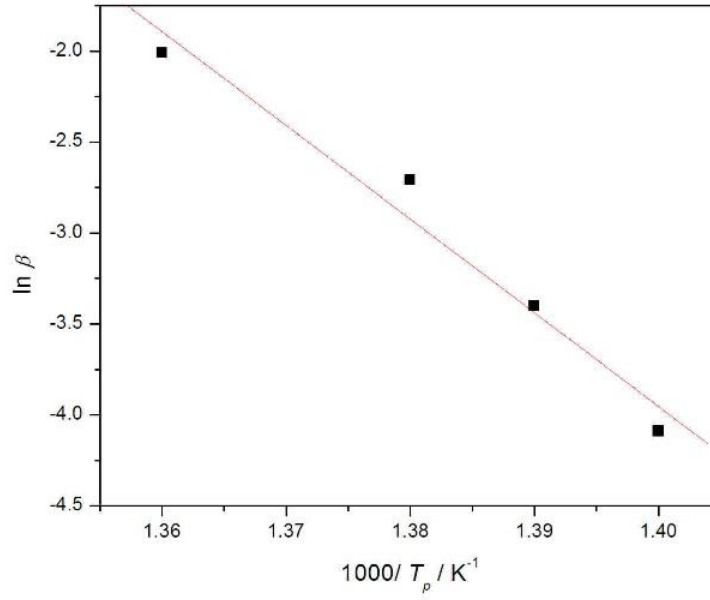


Fig. 3.8: Boswell plot; (a) Peak-1, (b) Peak-2

(a)



(b)

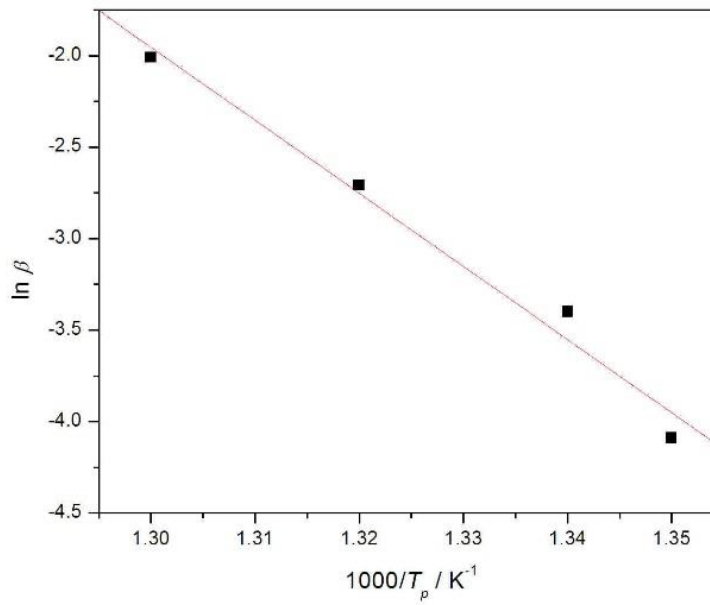


Fig. 3.9: Ozawa plot; (a) Peak-1, (b) Peak-2

Table 3.3 Activation energies ( $E$ ) and pre-exponential factor ( $k_0$ ) for different methods

Method	$E(\text{kJ/mol})$		$k_0 (\text{s}^{-1})$	
	Peak 1	Peak 2	Peak 1	Peak 2
Kissinger	$392 \pm 5$	$320 \pm 4$	$5.67 \times 10^{22}$	$3.93 \times 10^{16}$
Augis & Bennett's	$312 \pm 9$	$282 \pm 3$	$1.26 \times 10^{20}$	$1.38 \times 10^{17}$
Boswell	$398 \pm 5$	$324 \pm 4$	-	-
Ozawa	$383 \pm 7$	$316 \pm 5$	-	-
Gao & Wang	$385 \pm 4$	$306 \pm 1$	-	-

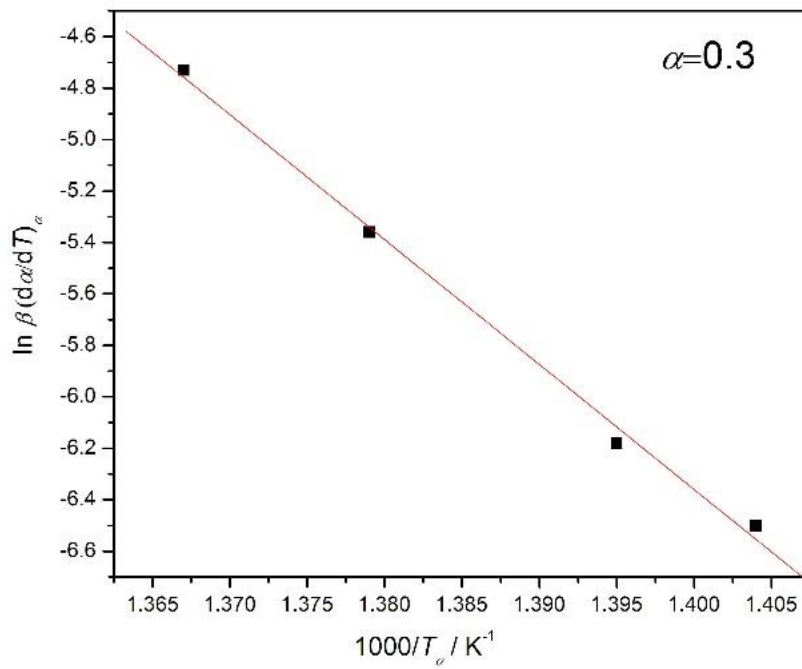
### 3.4.2 Linear Differential Iso-conversional Methods

---

Friedman [3.31] derived an expression for estimation of activation energy of crystallization based on the differential of the transformed fraction. Since it does not require any approximation for temperature integral, accurate results of  $E$  are expected to be obtained. The expression given by Friedman is shown in eq. (3.29). It provides variable value of  $E$  for different  $\alpha$ , that are reported in table 3.2. Fig. 3.10 shows a Friedman plot at  $\alpha=0.3$ .

A special case of Friedman's equation involves calculation of  $E$  only at  $T_p$ . This method was given by Gao and Wang [3.32]. Fig. 3.11 shows Gao and Wang plot obtained using eq. (3.31), and the so obtained values of  $E$  are reported in table 3.3.

(a)



(b)

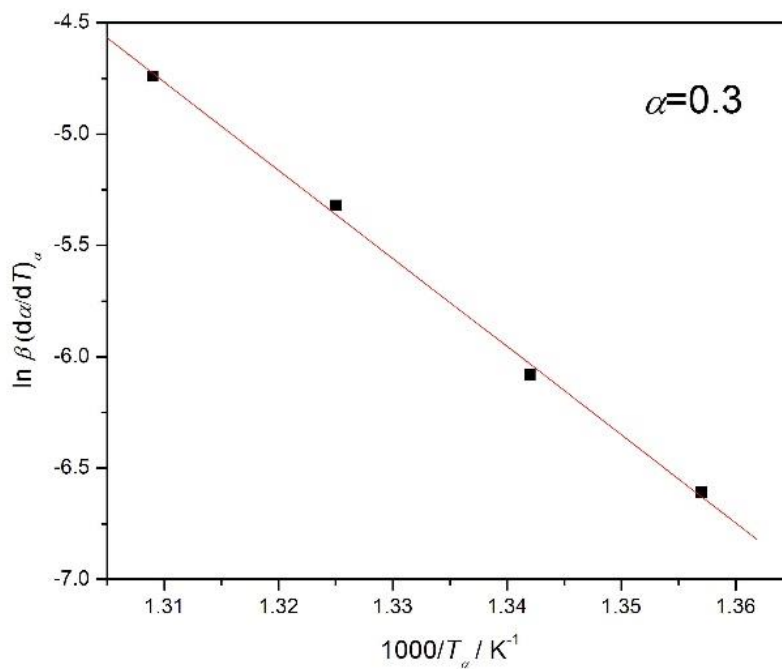
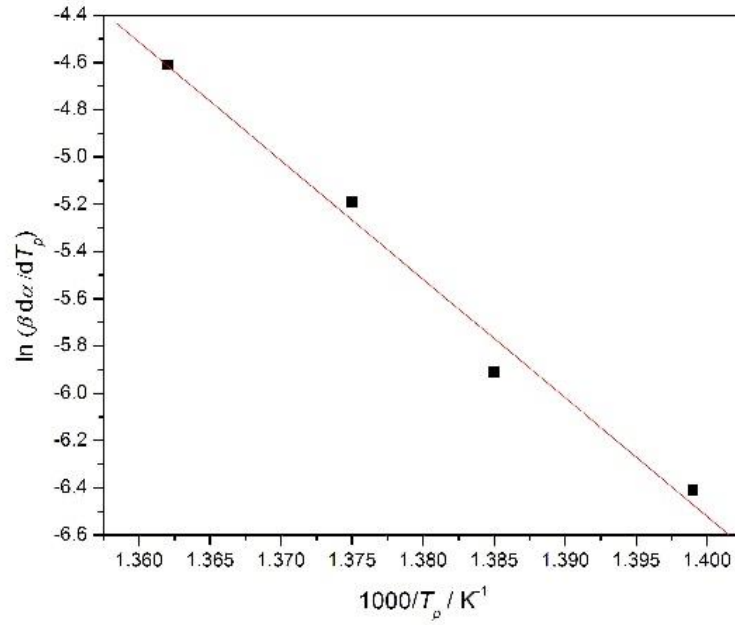


Fig. 3.10: Friedman plot for  $\alpha = 0.3$ ; (a) Peak-1, (b) Peak-2

(a)



(b)

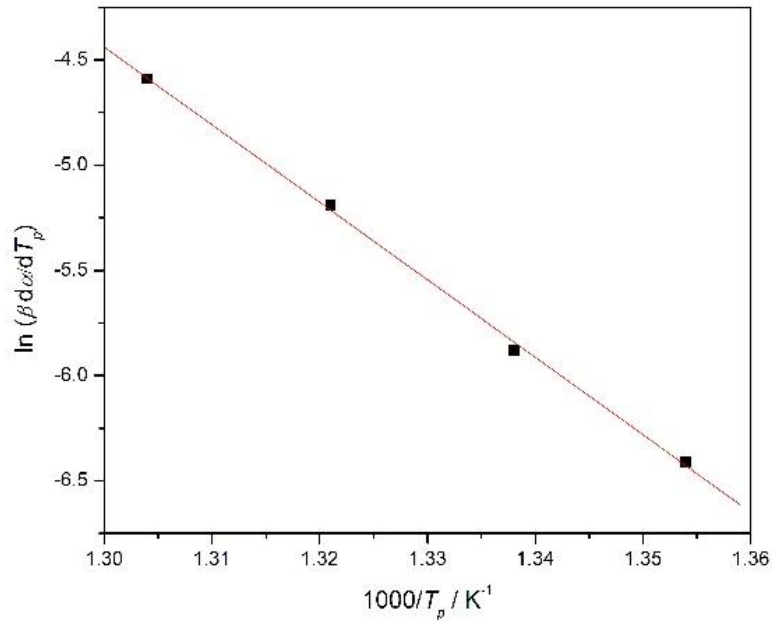
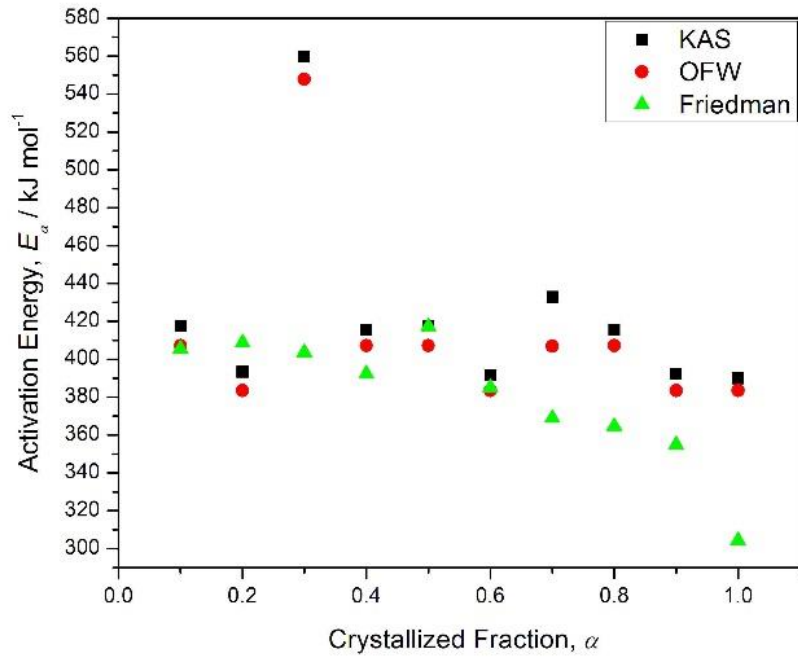


Fig. 3.11: Gao & Wang plot; (a) Peak-1, (b) Peak-2

(a)



(b)

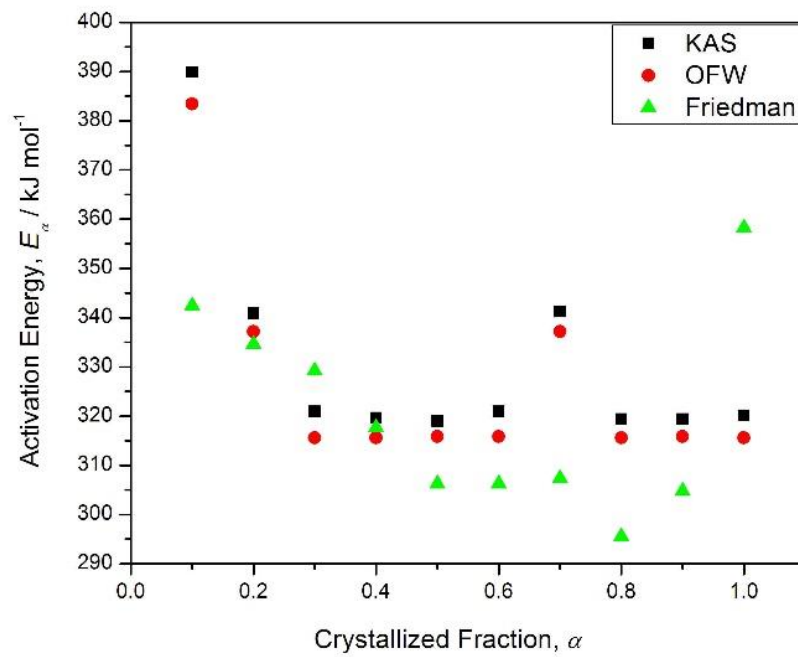


Fig. 3.12: Local activation energies ( $E_\alpha$ ) at different  $\alpha$  from different methods; (a) Peak-1, (b) Peak-2

The variation of local activation energies ( $E_\alpha$ ) with the crystallized fraction,  $\alpha$  has been shown in fig. 3.12(a) & fig. 3.12(b) respectively for peak-1 and peak-2 by using three different iso-conversional methods, namely KAS, OFW, and Friedman. The values of local activation energies ( $E_\alpha$ ) at different  $\alpha$ , are reported in table 3.2. For both the peaks KAS and OFW methods show similar variations in  $E_\alpha$  with  $\alpha$ , provided the  $E_\alpha$  values for OFW were smaller than that obtained by KAS method, whereas, Friedman points varied quite differently as compared to the KAS and OFW points.

For peak-1, all of the three methods show substantial variation with  $\alpha$ . KAS and OFW methods show a sudden increase in  $E_\alpha$  at  $\alpha=0.3$ . Then there is a decrease in  $E_\alpha$  values till  $\alpha=0.6$ , followed by a small increase at  $\alpha=0.7$  and then it further decreases, whereas Friedman points shows a continuous decrease till end except for  $\alpha=0.5$ . Therefore, the primary exothermic process can be interpreted as a multiple mechanism process. For peak-2,  $E_\alpha$  values obtained from KAS and OFW methods, first decreases from  $\alpha=0.1$  to  $\alpha=0.3$ , then remains almost constant from till  $\alpha=1$  except for a sudden increase at  $\alpha=0.7$ . The second exothermic event can also be explained in terms of a multiple step mechanism, since  $E_\alpha$  values varied considerably with  $\alpha$  for all three methods.

### **3.4.3 Heating Rate Dependence of Crystallization Temperatures**

---

The crystallization temperatures ( $T_x$  and  $T_p$ ) show a strong dependence on the heating rates employed.  $T_x$  and  $T_p$  get shifted to higher temperatures with an increase in heating rate employed [3.60-3.61]. Theoretically, the values of  $T_x$  and  $T_p$  for  $\text{Cu}_{60}\text{Zr}_{20}\text{Ti}_{20}$  metallic glass are calculated using eq. (3.47) and (3.49) respectively, and the efficacy of this relationship is confirmed by fitting it to the experimental values of  $T_x$  and  $T_p$  obtained using MDSC heating

experiments. Fig. 3.13 represents the variation of theoretically calculated  $T_x$  values with heating rate  $\beta$  for both the crystallization peaks. It can be seen that the calculated  $T_x$  values varies in accordance with the experimental  $T_x$  values. The variation of theoretically calculated and experimental  $T_p$  values is shown in figure-3.14, for both crystallization peaks. Both the calculated and experimental values of  $T_p$  are found to be in good agreement with each other. Hence, it can be understood that the power law equation is a suitable tool for understanding the variation of crystallization temperatures with heating rate. Using this concept of variation of  $T_x$  (or  $T_p$ ) with heating rate ( $\beta$ ), the activation energy for the crystallization of metallic glasses can be determined using different iso-kinetic and iso-conversional methods.

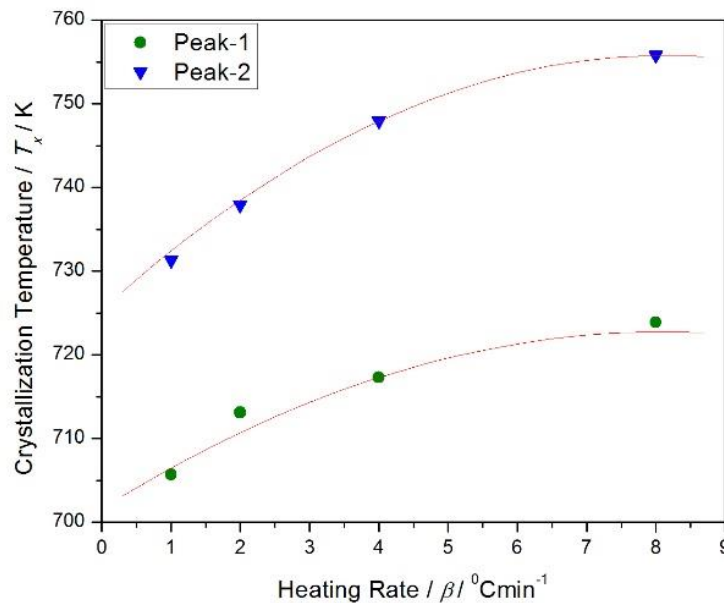


Fig. 3.13: Variation of onset of crystallization temperature ( $T_x$ ) with heating rate ( $\beta$ ): (—) represents theoretically calculated results using Eq. (3.47); (●, ▼) represents experimental points for peak 1 & 2 respectively for  $\text{Cu}_{60}\text{Zr}_{20}\text{Ti}_{20}$  metallic glass

$T_x$  and  $T_p$  are inversely proportional to the relaxation time which in turn varies inversely with heating rate ( $\beta$ ). Hence, with increase in heating rate,  $T_x$  and  $T_p$  increases. At smaller heating rates, the molecules get more time to relax and rearrange themselves into an ordered structure and hence the metallic glass starts crystallizing at a lower temperature, and vice-versa.

Another factor that affects the crystallization temperature of a metallic glass is the *atomic size mismatch*. A greater size mismatch among the constituent atoms is expected to cause to a higher value of  $T_x$ . Other factors responsible for variation in  $T_x$  includes reduction in free volume & diffusivity, electron to atom ratio and differences in electro-negativities.

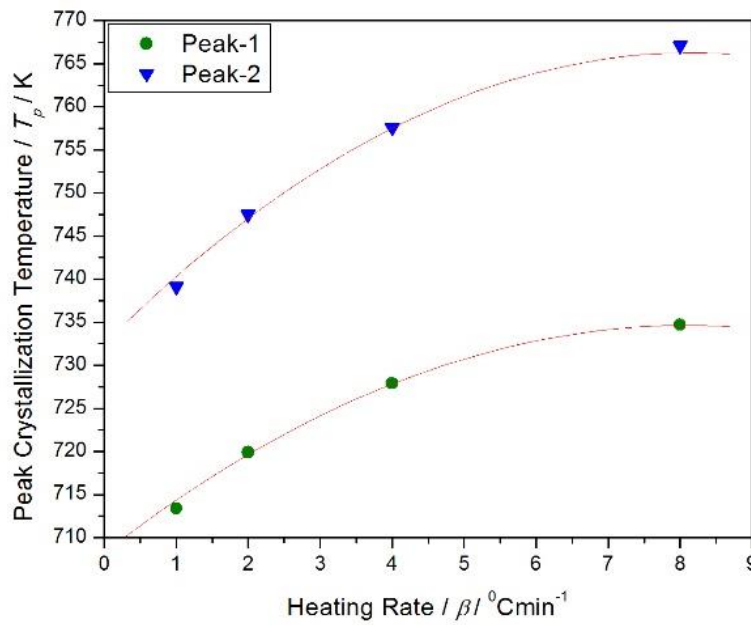


Fig. 3.14: Variation of peak crystallization temperature ( $T_p$ ) with heating rate ( $\beta$ ): (—) represents theoretically calculated results using Eq. (3.49); (●, ▼) represents experimental points for peak 1 & 2 respectively for  $\text{Cu}_{60}\text{Zr}_{20}\text{Ti}_{20}$  metallic glass

Table 3.4 Experimental  $T_x$  and  $T_p$  values at different heating rates for  $\text{Cu}_{60}\text{Zr}_{40}$  and  $\text{Cu}_{60}\text{Zr}_{20}\text{Ti}_{20}$  metallic glasses for peak 1

$\text{Cu}_{60}\text{Zr}_{40}$ [3.67]			$\text{Cu}_{60}\text{Zr}_{20}\text{Ti}_{20}$		
Heating rate ( $^{\circ}\text{Cmin}^{-1}$ )	$T_x$ (K)	$T_p$ (K)	Heating rate ( $^{\circ}\text{Cmin}^{-1}$ )	$T_x$ (K)	$T_p$ (K)
5	705.26	715.6	1	705.69	713.39
10	707.19	723	2	713.11	719.85
15	709.12	726.5	4	717.34	727.89
20	711.05	729.6	8	723.91	734.72

Table 3.4 represents experimental  $T_x$  and  $T_p$  values at different heating rates for  $\text{Cu}_{60}\text{Zr}_{40}$  and  $\text{Cu}_{60}\text{Zr}_{20}\text{Ti}_{20}$  metallic glasses. It can be observed that the characteristics temperatures shift towards higher values with increase in heating rates and number of components. A higher value of  $T_x$  represents greater GFA of metallic glass. In present case  $T_x$  value at  $\beta = 5^\circ\text{Cmin}^{-1}$  for binary system is equivalent to the value of  $T_x$  at  $\beta = 1^\circ\text{min}^{-1}$  for ternary system. This indicates that the substitution of Ti to the binary metallic glass shifts the value of  $T_x$  to a higher temperature. It implies that a ternary alloy is a better glass former as compared to its respective binary counterpart. Hence, the GFA of Cu-Zr binary alloy enhances significantly by the addition of Ti. Fig. 3.15 shows a linear variation of  $T_x$  and  $T_p$  with heating rate for  $\text{Cu}_{60}\text{Zr}_{40}$  metallic glass, given by the expression:

$$T_x \text{ (or } T_p) = A + B \beta \quad (3.51)$$

With  $A$  and  $B$  as the slope and intercept of the plot and  $\beta$  is the heating rate employed.

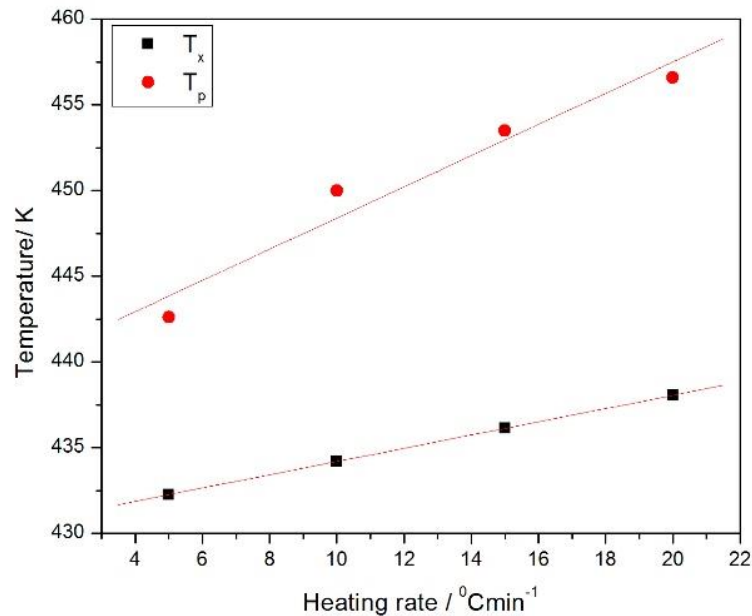


Fig. 3.15: Variation of  $T_x$  and  $T_p$  with heating rate for  $\text{Cu}_{60}\text{Zr}_{40}$  metallic glass [3.67]

Glass formation is favoured by the three empirical rules given by Inoue et al [3.68]: (i) number of components, (ii) size mis-match between the various components, and (iii) negative heat of mixing. More number of components makes the structure of glassy alloy denser and randomly packed with a short range order and thereby increases its GFA. Hence, ternary alloy  $\text{Cu}_{60}\text{Zr}_{20}\text{Ti}_{20}$  is a better glass former than  $\text{Cu}_{60}\text{Zr}_{40}$ . Secondly, the GFA of metallic glasses increases if the size difference between different components is more (>12%). With the addition of elements of different radii, it becomes difficult for the components to acquire their stable configuration due to increase in the entropy of disorder. In present case for  $\text{Cu}_{60}\text{Zr}_{20}\text{Ti}_{20}$  metallic glass, the atomic radius of Cu, Zr and Ti are 0.128 nm, 0.160 nm and 0.147 nm respectively. This size difference is sufficient to make the interchangeability between the different components difficult. Large size difference destabilizes the crystalline phase by increasing the internal energy of the crystalline solid solution. The prime root of metallic glass formation lies in destabilizing the competing crystalline phase. This destabilization of crystalline phase can be accomplished by atomic pair formation between unlike components with large size difference [3.69-3.71]. Formation of local crystalline structure, in alloys with same atomic sized components, is shown by Yun et al [3.71]. Hence, a greater GFA is crucially favoured by a large size mis-match and a large negative heat of mixing. The substitution of Zr by Ti makes the interchangeability among the components of the alloy easy, since Ti and Zr belong to the same group in periodic table and share common characteristics. Hence Ti becomes a suitable candidate for changing composition of metallic glass from  $\text{Cu}_{60}\text{Zr}_{40}$  to  $\text{Cu}_{60}\text{Zr}_{20}\text{Ti}_{20}$ . Thirdly, negative heat of mixing favours glass formation by coercing the formation of atomic pair between different components, which in turn increases the difficulty of atomic rearrangement in a glassy alloy during heating. The heats of mixing for atomic pairs Cu-Zr, Zr-Ti and Ti-Cu are -23, 0 and -9  $\text{kJ mol}^{-1}$  respectively [3.72]. These interactions are much weaker as compared to those atomic interactions in quaternary and quinary alloys such

as  $Zr_{55}Cu_{30}Al_{10}Ni_5$  and  $Zr_{41}Ti_{14}Cu_{12.5}Ni_{10}Be_{22.5}$ . The heats of mixing for atomic pairs in  $Zr_{55}Cu_{30}Al_{10}Ni_5$  and  $Zr_{41}Ti_{14}Cu_{12.5}Ni_{10}Be_{22.5}$  alloys are 0, -23, -49, -43, -44, -22, -9, -35 and -30  $\text{kJmol}^{-1}$  respectively for Zr-Ti, Zr-Cu, Zr-Ni, Zr-Be, Zr-Al, Al-Ni, Ti-Cu, Ti-Ni and Ti-Be [3.72]. These atomic interactions can also be understood in terms of pre-exponential factor ( $k_0$ ).  $k_0$  provides information about the number of jumps nuclei make per unit time in order to overcome the activation energy barrier. In general, it gives information about atomic mobility.  $k_0$  can be obtained by least square fitting of the crystallized fraction versus temperature curve. The values of  $k_0$  for first and second peaks, calculated by the iterative least-square fitting to the experimental data of fractional crystallization for  $Cu_{60}Zr_{20}Ti_{20}$  metallic glass, are found to be of the order  $10^{22}$  and  $10^{17} \text{ s}^{-1}$  respectively (table 3.1). Typical Zr based BMGs exhibit  $k_0$  of the order of  $10^{12} \text{ s}^{-1}$  for first crystallization peak, such as the value of  $k_0$  for  $Zr_{55}Cu_{30}Al_{10}Ni_5$  and  $Zr_{41}Ti_{14}Cu_{12.5}Ni_{10}Be_{22.5}$  BMGs are  $4.2 \times 10^{12} \text{ s}^{-1}$  and  $1.0 \times 10^{12} \text{ s}^{-1}$  respectively [3.60, 3.73]. This indicates that the value of  $k_0$  for  $Cu_{60}Zr_{20}Ti_{20}$  metallic glass is much higher than that of Zr-based quaternary and quinary BMGs. This may be due to the reason that quaternary and quinary BMGs are supposed to have higher degree of dense random packing as compared to that of the ternary alloy. Further  $k_0$  is greatly influenced by the configuration and atomic interactions between the various components of the alloy. The atoms of an alloy, with high degree of dense random packing, require greater energy to overcome the interatomic interactions. The mobility of atoms in alloys with strong interatomic interactions is less than the alloys with weak interatomic interactions. The heats of mixing of atomic pairs in quaternary and quinary BMGs are higher than that of the ternary alloy. Hence  $Zr_{55}Cu_{30}Al_{10}Ni_5$  and  $Zr_{41}Ti_{14}Cu_{12.5}Ni_{10}Be_{22.5}$  BMGs exhibit relatively smaller values of  $k_0$  as compared to  $Cu_{60}Zr_{20}Ti_{20}$  metallic glass.

## 3.5 Conclusions

### 3.5.1 Crystallization Kinetics of $\text{Ti}_{20}\text{Zr}_{20}\text{Cu}_{60}$ Metallic Glass

The non-isothermal crystallization kinetics for  $\text{Ti}_{20}\text{Zr}_{20}\text{Cu}_{60}$  metallic glass was studied by iso-conversional methods. The activation energy required for primary crystallization is found to be more than activation energy required for subsequent crystallization peak by all the iso-conversional methods. Iso-conversional methods provide values of activation energy,  $E_\alpha$  as a function of  $\alpha$ , which is not possible by any of the iso-kinetic methods. But the Avrami (growth) exponent that gives information about the dimensionality of crystal growth can be calculated by the use of iso-kinetic methods. Both methods of calculating the kinetic parameters for crystallization process provide fairly accurate results near peak crystallization temperature as seen from fig. 3.3 (a) - (h). Though fig 3.1 shows that iso-kinetic method provides better fitting to the experimental  $\alpha$  value, but the complexity of crystallization event can be better understood by iso-conversional methods. Hence, the combination of both methods can be used for studying the kinetics of crystallization process. KAS, OFW, and Friedman methods provide activation energies dependent on  $\alpha$ . The values of  $E_\alpha$  obtained by KAS and OFW methods lie close to each other, whereas Friedman method shows a different variation of  $E_\alpha$  with  $\alpha$ . For peak-1,  $E_\alpha$  values show an irregular variation with  $\alpha$ . For peak-2 also there is a substantial decrease in  $E_\alpha$ , from  $\alpha = 0.1$  to  $\alpha = 0.3$ . Afterwards, it remains constant except for  $\alpha = 0.7$ . Hence, both crystallization events are multiple mechanism processes. Also, the term that is expected to cause non-linearity, i.e.,  $(A_T\omega/2\beta)^2$  is almost constant for all heating rates. Thus, the non-linear heating rate does not change the nature of different linear iso-conversional methods. The linear behaviour of the various expressions remains intact. Hence, MDSC can be conveniently used for studying kinetics of crystallization of metallic glasses.

### 3.5.2 Heating Rate Dependence of Crystallization Temperatures

---

In order to study the stability of metallic glasses, it is required to understand their behaviour towards crystallization event. Crystallization is characterized by the onset of crystallization temperature ( $T_x$ ) and peak crystallization temperature ( $T_p$ ). This study provides an insight of heating rate and composition dependence of crystallization temperature. Both The crystallization temperature ( $T_x$ ) and the peak crystallization temperature ( $T_p$ ) are found to follow a power law variation with heating rate for  $\text{Cu}_{60}\text{Zr}_{20}\text{Ti}_{20}$  metallic glass. It also provides information about the heating rate suitable for crystallization of a melts. In absence of sufficient experimental data one can make use of theoretical formulae for deriving useful conclusions regarding the kinetics of crystallization.  $\text{Cu}_{60}\text{Zr}_{40}$  binary alloy follows a linear variation for both the characteristic temperatures i.e.,  $T_x$  and  $T_p$  respectively. Further, an addition of Ti to binary alloy increases the characteristic temperatures, which enhances the GFA. Hence, an increase in number of components increases the GFA of a metallic glass.

## References

---

- [3.1] L. Wilhelmy, 1891, *Ostwalds Klassiker der exakten Wissenschaften*, No. 29, edited by W. Ostwald. (Leipzig: Verlag von Wilhelm Engelmann), p. 1.
- [3.2] C. M. Guldberg and P. Waage, 1899, *Ostwalds Klassiker der exakten Wissenschaften*, No. 104, edited by W. Ostwald. (Leipzig: Verlag von Wilhelm Engelmann), p. 1.
- [3.3] J. H. van't Hoff, 1884, *Etudes de Dynamique Chimique* (Amsterdam: Frederik Muller).
- [3.4] W. Ostwald, 1894, *Manual of Physico-chemical Measurements* (London: Macmillan), p. 246.
- [3.5] G. N. Lewis, *Z. phys. Chem.* **52**; 1905: 310.
- [3.6] J. Y. MacDonald J. Y. and C. N. Hinshelwood, *J. chem. Soc.* **128**; 1925: 2764.
- [3.7] B. Bruzs, *J. phys. Chem.*, **30**; 1926: 680.
- [3.8] W. E. Garner and H. R. Hailes, *Proc. R. Soc. A*, **139**; 1933: 576.
- [3.9] Ch. Bagdassarian, *Acta Physicochim. URSS*, **20**; 1945: 441.
- [3.10] B. V. Erofeev, *Ct. rd. Acad. Sci. URSS*, **52**; 1946: 511.
- [3.11] A. R. Allnatt and P. W. M. Jacobs, *Can. J. Chem.* **46**; 1968: 111.
- [3.12] P. W. M. Jacobs and F. C. Tompkins, *Chemistry of the Solid State* edited by W. E. Garner (London: Butterworth), 1955, p. 187.
- [3.13] M. E. Brown, D. Dollimore and A. K. Galwey, *Reactions in the Solid State. Comprehensive Chemical Kinetics*, Vol. 22. Amsterdam: Elsevier. 1980, 340 pp.
- [3.14] T. B. Brill and K. J. James, *Chem. Rev.* **93**; 1993: 2667–92
- [3.15] J. H. Flynn, In *Encyclopedia of Polymer Science and Engineering*, ed. HF Mark, NM Bikales, CG Overberger, G Menges, 1989, pp. 690–723 (Suppl.). New York: Wiley

- [3.16] D. W. Van Krevelen, *Coal. Typology Physics - Chemistry - Constitution*. Amsterdam: Elsevier, 1993
- [3.17] J. Sestak, *Thermophysical Properties of Solids. Comprehensive Analytical Chemistry*, Vol. 12D. Amsterdam: Elsevier. 1984: pp 440.
- [3.18] J. G. Fatou, In *Encyclopedia of Polymer Science and Engineering*, ed. HF Mark, NM Bikales, CG Overberger, G Menges, 1989, pp. 231–96 (Suppl.). New York:Wiley
- [3.19] J. H. Peperzko, In *Thermal Analysis in Metallurgy*, ed. RD Schull, A Joshi, 1992, pp.121–53. Warrendale, PA: TMS
- [3.20] D. Dollimore, *Anal. Chem.* **68**; 1996: R63–R71
- [3.21] S. Arrhenius, *Z. phys. Chem.*, **4**; 1889: 226.
- [3.22] C. N. Hinshelwood, *The Kinetics of Chemical Change in Gaseous Systems* (London: Oxford University Press). 1926
- [3.23] S. Vyazovkin and C. A. Wight, *Annu. Rev. Phys. Chem.* **48**; 1997: 125.
- [3.24] S. Vyazovkin and D. Dollimore, *J. Chem. Inf. Comput. Sci.* **36** (1); 1996: 42.
- [3.25] T. Ozawa, *Bull. Chem. Soc. Jpn.***38**; 1965: 1881.
- [3.26] J. H. Flynn and L. A. Wall, *J. Res. Natl. Bur. Stand. A. Phys. Chem.***70A**; 1966: 487.
- [3.27] H. E. Kissinger, *Anal. Chem.* **29**; 1966: 1702.
- [3.28] T. Akahira and T. Sunose, *Research report (Chiba Institute of Technology) Sci Technol.***16**; 1971: 22.
- [3.29] A. Augis and J. E. Bennett, *J. Therm. Anal. Calorim.* **13**; 1978: 283.
- [3.30] P. G. Boswell, *J. Therm. Anal. Calorim.* **18**; 1980: 353.
- [3.31] H. L. Friedman, *J. Polym. Sci.* **C6**; 1964: 183.
- [3.32] Y. Q. Gao and W. Wang, *J. Non. Cryst. Solids.* **81**; 1986: 129.
- [3.33] J. Malek, *Thermochim. Acta.* **267**; 1995: 61.
- [3.34] F. J. Gotor, J. M. Criado, J. M. Malek and N. Koga, *J. Phys. Chem. A.* **104**; 2000: 10777

- [3.35] F. Paulik, Ch.10: Special Trends in Therm. Anal. John Wiley & Sons, Chichester, UK, (1995).
- [3.36] S. Vyazovkin and C. A. Wight, *Thermochim. Acta.* **340-341**; 1990: 53.
- [3.37] A. K. Burnham and L. N. Dinh, *J. Therm. Anal. Calorim.* **89(2)**; 2007: 479.
- [3.38] M. J. Starnik, *Thermochim. Acta.* **404**; 2003: 163.
- [3.39] A. Pratap, T. L. S. Rao, K. N. Lad and H. D. Dhurandhar, *J. Therm. Anal. Calorim.* **89(2)**; 2007: 399.
- [3.40] C. Pacurariu and I. Lazau, *J. Non-Cryst. Solids.***358**; 2012: 3332.
- [3.41] A. W. Coats and J. P. Redfern, *Nature (London)* **201**; 1964: 68.
- [3.42] A. Pratap and K. Sharma, *J. Therm. Anal. Calorim.* **107(1)**; 2012: 171.
- [3.43] C. D. Doyle, *J. Appl. Polym. Sci.* **5**; 1961: 285.
- [3.44] C. D. Doyle, *J. Appl. Polym. Sci.* **6**; 1962: 642.
- [3.45] C. D. Doyle, *Nature (London)* **207**; 1965: 290.
- [3.46] A. N. Kolmogorov, *Bull. Acad. Sci. USSR Phys. ser.* **3**; 1937: 555.
- [3.47] W. A. Johnson and P. A. Mehl, *Trans. Am. Inst. Min. Metall. Eng.* **135**; 1939: 416.
- [3.48] M. Avrami, *J. Chem. Phys.* **7(12)**; 1939: 1103.
- [3.49] M. Avrami, *J. Chem. Phys.* **8(2)**; 1940: 212.
- [3.50] M. Avrami, *J. Chem. Phys.* **9(2)**; 1941: 177.
- [3.51] N. S. Mohan and R. Chen, *J. Phys. D: Appl. Phys.* **3**; 1970: 243.
- [3.52] W. Tang, Y. Liu, H. Zhang and C. Wang, *Thermochim. Acta.* **408**; 2003: 39.
- [3.53] V. M. Gorbachev, *J. Therm. Anal.* **8**; 1975: 349.
- [3.54] D. W. Henderson, *J. Non-cryst. solids.* **30**; 1979: 301.
- [3.55] J. Malek, *Thermochim. Acta.***355**; 2000: 239.
- [3.56] J. Šesták and G. Berggren, *Thermochim. Acta*, **3**; 1971: 1.
- [3.57] W. Lu, B. Yan and W. Huang, *J. non-cryst. solids.* **351**; 2005: 3320.

- [3.58] S. R. Joshi, A. Pratap, N. S. Saxena, M. P. Saksena and A. Kumar, *J. Mater. Sci Lett.* **13**; 1994: 77.
- [3.59] M. Lasocka, *Mater. Sci. Eng. A.* **23**; 1976: 173.
- [3.60] L. Liu, Z. F. Wu and J. Zhang, *J. Alloys Compd.* **339**; 2002: 90.
- [3.61] X. Ou, G. Q. Zhang, X. Xu, L. N. Wang, J. H. Liu and J. Z. Jiang, *J. Alloys Compds.* **441**; 2007: 181.
- [3.62] A. Inoue, W. Zhang, T. Zhang and K. Kurosaka, *Mater. Trans. JIM.* **42**; 2001: 1149.
- [3.63] Y. K. Kovneristyj and A. G. Pashkovskaya, *Amorf. (Stekloobraz) Met. Mater. RAN Int. Metallurgii. M.* 1992; p153-157
- [3.64] S. Kasyap, A. T. Patel and A. Pratap, *J. Therm. Anal. Calorim.* **116**; 2014: 1325.
- [3.65] A. Pratap, K. N. Lad, R. T. Savaliya, G. K. Dey, S. Banerjee and A. M. Awasthi, *Phys. Chem. Glasses.* **45**; 2004: 258.
- [3.66] A. Pratap, K. G. Raval and A. Gupta, *Proc. 11th Nat. Symp. on Therm. Anal.* 1998; pp.22-24.
- [3.67] G. D. Ladiwala, N. S. Saxena, S. R. Joshi, A. Pratap and M. P. Saksena, *Mater. Sci. Engg. A.* **A181/A182**; 1994: 1427.
- [3.68] A. Inoue, A. Takeuchi and T. Zhang, *Metall. Mater. Trans. A.* **29**; 1998: 1779.
- [3.69] O. N. Senkov and D. B. Miracle, *Mater. Res. Bull.* **36**; 2001: 2183.
- [3.70] Z. P. Lu, C. T. Liu and Y. D. Dong, *J. Non-Cryst. Solids.* **341**; 2004: 93.
- [3.71] Y. S. Yun, H. S. Nam, P. R. Cha, W. T. Kim and D. H. Kim, *Met. Mater. Int.* **20**; 2014: 105.
- [3.72] A. Takeuchi and A. Inoue, *Mater. Trans. JIM.* **41**; 2000: 1372.
- [3.73] Y. X. Zhuang, W. H. Wang, Y. Zhang, M. X. Pan and D. Q. Zhao, *Appl. Phys. Lett.* **75**; 1999: 2392.